

1 **Title: A novel bacterial protease inhibitor adjuvant in RBD-based COVID-19 vaccine**  
2 **formulations increases neutralizing antibodies, specific germinal center B cells and confers**  
3 **protection against SARS-CoV-2 infection.**

4

5 **Authors:**

6 Lorena M. Coria<sup>a</sup>, Lucas M. Saposnik<sup>a§</sup>, Celeste Pueblas Castro<sup>a§</sup>, Eliana F. Castro<sup>a,b§</sup>, Laura A.  
7 Bruno<sup>a</sup>, William B. Stone<sup>c</sup>, Paula S. Pérez<sup>d</sup>, M. Laura Darriba<sup>a</sup>, Lucia B. Chemes<sup>a</sup>, Julieta Alcain<sup>a</sup>,  
8 Ignacio Mazzitelli<sup>d</sup>, Augusto Varese<sup>d</sup>, Melina Salvatori<sup>d</sup>, Albert J. Auguste<sup>c,e</sup>, Diego E Álvarez<sup>a</sup>,  
9 Karina A. Pasquevich<sup>a\*†</sup> and Juliana Cassataro<sup>a\*</sup>

10

11 **Author Affiliations:**

12 <sup>a</sup> Instituto de Investigaciones Biotecnológicas Dr. Rodolfo A. Ugalde, Universidad Nacional de  
13 San Martín, Consejo Nacional de Investigaciones Científicas y Técnicas (UNSAM-CONICET),  
14 San Martín (1650), Buenos Aires, Argentina.

15 <sup>b</sup> Instituto de Virología e Innovaciones Tecnológicas (IVIT), Centro de Investigaciones en Ciencias  
16 Veterinarias y Agronómicas (CICVyA), Instituto Nacional de Tecnología Agropecuaria (INTA)-  
17 Consejo Nacional de Investigaciones Científicas y Técnicas (CONICET), Buenos Aires,  
18 Argentina.

19 <sup>c</sup> Department of Entomology, College of Agriculture and Life Sciences, Fralin Life Science  
20 Institute, Virginia Polytechnic Institute and State University, Blacksburg, VA, 24061.

21 <sup>d</sup> Instituto de Investigaciones Biomédicas en Retrovirus y SIDA (INBIRS, Universidad de Buenos  
22 Aires - CONICET), Buenos Aires, Argentina.

23 <sup>e</sup> Center for Emerging, Zoonotic, and Arthropod-borne Pathogens, Virginia Polytechnic Institute  
24 and State University, Blacksburg, VA, 24061.

25

26 **Corresponding Author:** \*Address correspondence to Karina A. Pasquevich  
27 [kpasquevich@iibintech.com.ar](mailto:kpasquevich@iibintech.com.ar) and to Juliana Cassataro: [jucassataro@iib.unsam.edu.ar](mailto:jucassataro@iib.unsam.edu.ar)

28

29 <sup>†</sup> K.A.P. and J.C. contributed equally to this work.

30 <sup>§</sup> L.M.S., C.P.C. and E.F.C. contributed equally to this work.

31

32 **Running title:** A novel bacterial adjuvant in RBD-based COVID-19 vaccine

33

34 **Abstract**

35           In this work we evaluated recombinant receptor binding domain (RBD) based vaccine  
36 formulation prototypes with potential for further clinical development. We assessed different  
37 formulations containing RBD plus Alum, AddaS03, AddaVax or the combination of Alum and U-  
38 Omp19: a novel *Brucella* spp. protease inhibitor vaccine adjuvant. Results show that the vaccine  
39 formulation composed of U-Omp19 and Alum as adjuvants have a better performance: it  
40 significantly increased mucosal and systemic neutralizing antibodies in comparison to antigen plus  
41 Alum, AddaVax or AddaS03. Antibodies induced with the formulation containing U-Omp19 not only  
42 increased their neutralization capacity against the wild-type virus but also cross neutralized alpha,  
43 lambda and gamma variants with similar potency. Also, addition of U-Omp19 to vaccine formulation  
44 increased the frequency of RBD-specific germinal center B cells and plasmablasts. Additionally, U-  
45 Omp19+Alum formulation induced RBD-specific Th1 and CD8<sup>+</sup> T cell responses in spleens and  
46 lungs. Finally, this vaccine formulation conferred protection against an intranasal SARS-CoV-2  
47 challenge of K18-hACE2 mice.

48

## 49 **Introduction**

50 Severe acute respiratory syndrome coronavirus 2 (SARS-CoV-2) is the causative agent of  
51 coronavirus disease 2019 (COVID-19) that developed into a global pandemic causing (as of  
52 November 30, 2021) over 260 million cases and over 5.2 million deaths worldwide (Weekly  
53 epidemiological update, World Health Organization, WHO). Mass vaccination offers the most  
54 efficient public health intervention to control the pandemic. Several vaccines have been shown to be  
55 effective and have been either approved or authorized for emergency use in different countries  
56 (Status of COVID-19 Vaccines,WHO).

57 Despite the efforts made to vaccinate people, it is still too early to establish the durability and  
58 extent of protection, and recent data on approved vaccines have showed a diminished efficacy six  
59 months after vaccination<sup>1-3</sup>. Most importantly, it is critical to find a way to optimize the existing  
60 vaccines to protect against the prevalent SARS-CoV-2 variants of concern (VOC) that are spreading  
61 globally<sup>4</sup>. Evidence of waning immunity and viral diversification create a possible need for a booster  
62 vaccine dose to protect the population<sup>5</sup> leading advisory health agencies to recommend and  
63 additional dose of a COVID-19 vaccine. For all these reasons, there is a need to produce safer,  
64 more effective, highly scalable, and more affordable COVID-19 vaccines locally or regionally.

65 Most of the approved vaccines are mRNA-based, vector-based or inactivated viruses.  
66 Currently, there are a few protein-based subunit vaccine candidates in late phase trials<sup>6</sup>. Subunit  
67 vaccines are a well-known platform, and many subunit vaccines are already in widespread use.  
68 Protein subunit vaccines are easy to produce and safe, but in practice, they require a suitable  
69 adjuvant to stimulate the host immune response.

70 Subunit vaccine candidates in development are mainly based on Spike protein or the SARS-  
71 CoV-2 receptor-binding domain (RBD). RBD is located within the S1 subunit of the Spike.  
72 Angiotensin converting enzyme 2 (ACE2) is the functional receptor for SARS-CoV-2 comprising a  
73 critical factor for SARS-CoV-2 to enter into target cells and RBD is a key functional component that  
74 is responsible for binding of SARS-CoV-2 to host cells<sup>7,8</sup>. It is therefore not surprising that antibodies  
75 directed against the RBD or overlapping with the ACE2 binding region are strongly neutralizing,

76 making the RBD a promising subunit vaccine candidate<sup>9</sup>. RBD-based antigens have been described  
77 in previous studies for SARS-CoV and MERS-CoV vaccine development<sup>9,10</sup>. RBD from SARS-CoV-  
78 2 is an ideal antigen for vaccine formulations because of its high expression levels, ease of  
79 manufacturing, stability, and capacity to elicit functional antibodies<sup>11</sup>.

80 Although there is not a defined immune correlate of protection from SARS-CoV-2 infection  
81 yet, it has been proposed that neutralizing antibody levels are highly predictive of immune  
82 protection<sup>12,13</sup>. It has been found a strong correlation between vaccine-induced neutralizing  
83 antibodies (nAbs) and a reduction of viral loads in non-human primates and humans after SARS-  
84 CoV-2 infection<sup>14,15</sup>. T cell responses also play important protective roles in SARS-CoV-2 infection.  
85 The depletion of T cells in rhesus macaques has been shown to impair virus clearance<sup>14</sup>. In  
86 humans, virus-specific CD4<sup>+</sup> and CD8<sup>+</sup> T cell responses are associated with milder disease,  
87 indicating an involvement in protective immunity against COVID-19. Therefore, an ideal vaccine is  
88 expected to induce both the humoral and cellular arms of the immune system.

89 Vaccine adjuvants can enhance the magnitude, breadth, and durability of the immune  
90 response. Following its introduction in the 1920s, alum remained the only adjuvant licensed for  
91 human use for the next 70 years, however, five new adjuvants have been included in licensed  
92 vaccines until present<sup>16</sup>. The design and selection of adjuvants for COVID-19 vaccine formulations  
93 are key to induce optimal immune responses with adequate safety profiles. The introduction of  
94 novel adjuvants which have been shown to induce both humoral and cellular immune responses  
95 could be more favorable.

96 In previous works we demonstrated that a bacterial protease inhibitor from *Brucella abortus*  
97 (U-Omp19) can be used as an adjuvant in parenteral and oral vaccine formulations<sup>17-20</sup>. U-Omp19  
98 parenteral delivery induces the recruitment of CD11c<sup>+</sup> CD8α<sup>+</sup> dendritic cells (DCs) and monocytes  
99 to lymph nodes where it partially limits *in vivo* antigen (Ag) proteolysis inside DCs and increases Ag  
100 intracellular half-life. Consequently, U-Omp19 enhances Ag cross-presentation by DCs to CD8<sup>+</sup> T  
101 cells. Antitumor responses were elicited after U-Omp19 co-administration, increasing survival of  
102 mice in a murine melanoma challenge model. Moreover, subcutaneous, or intramuscular co-

103 administration of U-Omp19 with *Trypanosoma cruzi* Ags conferred protection against virulent  
104 parasite challenge, reducing parasitemia and increasing mice survival<sup>19,21</sup>. When U-Omp19 was co-  
105 delivered orally it increased mucosal Th1, Th17, CD8 T and Ab responses and reduced parasite or  
106 bacterial loads after oral challenge with virulent *Toxoplasma gondii* or *Salmonella*<sup>20</sup>. Thus, U-Omp19  
107 is a promising novel adjuvant able to promote specific Th1 and CD8<sup>+</sup> T cell immune responses in  
108 addition to Ab responses.

109 Here, we present preclinical data of a COVID-19 recombinant RBD-based vaccine candidate  
110 formulated with Alum and U-Omp19 adjuvant with potential for further clinical development.  
111 Development of recombinant protein based COVID-19 vaccines could allow vaccine availability  
112 even in low- and middle-income countries at affordable costs.

113

## 114 RESULTS

### 115 *Antigen expression and characterization*

116 In this study, RBD was used as the vaccine antigen. A monomeric version of RBD preceded  
117 by SARS-CoV-2 spike signal peptide for secretion and a C- terminal hexahistidine (6xHis)-Tag was  
118 expressed after plasmid transfection in HEK-293 cells. The RBD segment selected in this study  
119 (residues 319-341) contains 8 predicted immunodominant CD4<sup>+</sup> T cell epitopes and 17 predicted  
120 CD8<sup>+</sup> T cell epitopes in addition to B cell epitope motifs<sup>22</sup>.

121 Recombinant RBD was purified from cell culture supernatant through a single-step Ni-NTA  
122 affinity chromatography. SARS-CoV-2 RBD protein had high expression with remarkable purity (**Fig.**  
123 **1A**). Noteworthy, purified RBD was recognized by polyclonal antibodies in sera from a convalescent  
124 patient infected with SARS-CoV-2 (**Fig. 1B**). Analytical evaluation by size exclusion chromatography  
125 revealed that the recombinant protein is monodispersed. The sample eluted as a single peak with  
126 an apparent molecular weight of 40.3 KDa, representing >95% of the sample. (**Fig. 1C**). Endotoxin  
127 levels measured in the purified protein were ≤1,25EU per mg, this value is significantly lower than  
128 the maximum recommended endotoxin level for recombinant subunit human vaccines<sup>23</sup>.

129 Purified RBD was also assessed for its direct binding to the human ACE2 receptor in ACE2-  
130 expressing HEK-293T cells by flow cytometry. Strong binding of recombinant RBD to hACE2-HEK-  
131 293T cells was evidenced (>90%) (**Fig. 1D**). This result confirms that purified RBD binds to cell-  
132 associated hACE2 receptor suggesting that it has a correct folding.

### 133 *All vaccine formulations induce serum RBD specific IgG responses while only U-* 134 *Omp19+RBD+Alum formulation induces specific IgA in BAL after intramuscular* 135 *immunization*

136 The immunogenicity of a variety of vaccine formulations comprising recombinant RBD with  
137 different adjuvants was evaluated in mice. We assessed formulations containing approved  
138 adjuvants for human use, including Aluminium hydroxide, AddaS03 (similar to MF59) or AddaVax  
139 (similar to AS03) and the combination of Alum and U-Omp19, a novel adjuvant developed in our

140 laboratory that demonstrated vaccine adjuvant properties when co-administered with different Ags  
141 at pre-clinical stages.

142 Recombinant RBD was formulated with aluminium hydroxide (-Alum- Alhydrogel 2%) alone,  
143 Alum plus U-Omp19, AddaS03 or AddaVax. BALB/c mice received two doses at day 0 and 14 via  
144 intramuscular (i.m.) route (**Fig. 2A**). After the first dose, animals immunized with RBD+Alum or  
145 RBD+Alum+U-Omp19 produced a specific anti-RBD IgG response in serum (GMT at day 14: 4222  
146 and 5572 respectively, **Fig. 2B**). Anti-RBD IgG titers increased after the second dose reaching a  
147 plateau (GMT at day 42: 215269 and 323050 respectively, **Fig. 2B**). The groups of animals  
148 immunized with formulations containing AddaVax or AddaS03 as adjuvants failed to induce specific  
149 antibodies after the first dose (**Fig. 2B**) but showed a significant anti-RBD IgG response after two  
150 doses (GMT at day 42: 337794 and 215269 respectively). RBD-specific IgG subclasses were  
151 evaluated one month after last immunization demonstrating that all vaccine formulations induced  
152 higher titers of IgG1 than IgG2a in serum of mice (**Fig. 2C**). Specific-IgA at the low respiratory tract  
153 has an important role to control virus dissemination<sup>24</sup>. Interestingly, levels of RBD-specific IgA in the  
154 bronchoalveolar lavage (BAL) of mice were higher in the group that received RBD+Alum+U-Omp19  
155 than in groups that received AddaVax or AddaS03 (**Fig. 2D**). Besides, anti-RBD IgA was measured  
156 in serum samples revealing that groups containing Alum or Alum plus U-Omp19 as adjuvants  
157 induced significant higher levels compared to PBS or groups containing AddaVax or AddaS03 as  
158 adjuvants (**Fig. 2E**).

159 ***U-Omp19+Ag+Alum formulation significantly increases mucosal and systemic neutralizing***  
160 ***Abs in comparison to Ag plus Alum, AddaVax or AddaS03***

161 Next, the neutralization capacity of the vaccine induced antibodies was evaluated using an  
162 HIV-based pseudovirus neutralization assay (PsVNA). All vaccine formulations induced serum  
163 neutralizing antibodies against the SARS-CoV-2 spike pseudotyped virus (**Fig. 3A**). Remarkably,  
164 immunization with two doses of the formulation containing Alum plus U-Omp19 as adjuvants  
165 induced a ten-fold increase in the neutralization titer (GMT 325.1 95%CI 103.8-1018) compared to  
166 the groups immunized with Alum alone as adjuvant, AddaVax or AddaS03 (GMT 34.2 95%CI 3.790-

167 308.5, **Fig. 3A**). This increment was statistically significant ( $p=0.0257$  vs RBD+Alum,  $p =0.0259$  vs  
168 AddaVax and  $p =0.022$  vs AddaS03). AddaVax or AddaS03 as adjuvants induced a titer of  
169 neutralizing antibodies similar to Alum alone (**Fig. 3B**).

170 To assess the functionality of vaccine-elicited antibodies against the wild-type SARS-CoV-2,  
171 neutralization assay with sera from immunized animals was performed. Similar to the results  
172 obtained using the pseudovirus system, one month after the second dose, RBD+Alum+U-Omp19  
173 immunized mice had significant higher virus neutralization antibody titers in serum (**Fig. 3C**, GMT  
174 612.1 95%CI 87.80-4267) than mice immunized with RBD+Alum (**Fig. 3C**, GMT 140 95%CI 16.34-  
175 1199) or plus commercial adjuvants (AddaVax or AddaS03). These results further confirm the data  
176 obtained by PsVNA.

177 As SARS-CoV-2 initially infects the upper respiratory tract, its first interactions with the  
178 immune system must occur predominantly at the respiratory mucosal surfaces. Mucosal responses  
179 may be crucial to stop person to person transmission of this virus. Thus, examination of neutralizing  
180 activity in BAL was performed using pseudotyped virus system. Of note, adding U-Omp19 as an  
181 adjuvant to the formulation increased wild-type virus neutralization in the BAL of mice compared  
182 with the vaccine adjuvanted with Alum alone, AddaVax or AddaS03 (**Fig. 3D**,  $*p<0.05$ ).

### 183 ***Neutralizing antibodies last over 5-6 months after immunization with U-Omp19+Ag+Alum***

184 Duration of vaccine immunity is key to estimate how long protection lasts. To this effect, we  
185 evaluated the level of total antibodies over 175 days after prime immunization with the vaccine  
186 formulation containing U-Omp19 and alum as adjuvants. Interestingly, titers of anti-RBD IgG  
187 antibodies remained stable at least 5-6 months after i.m. immunization of mice with this formulation  
188 (**Fig. 4A**). Remarkably, neutralizing capacity of the antibodies remained stable till day 175 post  
189 prime immunization (**Fig. 4B**)

### 190 ***U-Omp19+Ag+Alum formulation induces neutralizing Abs against multiple SARS-CoV-2*** 191 ***variants***



192 To adequately address the public health impact that newly emerging COVID-19 variants  
193 present, there is a need for vaccine-elicited antibodies that can cross-neutralize different SARS-  
194 CoV-2 variants. Thus, neutralization activity of sera against prevalent circulating variants of SARS-  
195 CoV-2 in our region: alpha (B.1.1.7, first identified in UK), gamma (P.1, first identified in Manaus,  
196 Brazil) and lambda (C.37, first identified in Peru) was evaluated and compared to neutralizing  
197 activity against wild-type reference strain. In particular, gamma and lambda variants have been  
198 shown to partially escape neutralization by antibodies triggered by previously circulating variants or  
199 vaccine induced antibodies<sup>25,26</sup>. Noteworthy, antibodies induced after vaccination with the  
200 formulation containing U-Omp19 not only neutralize the wild-type virus but also cross neutralized  
201 alpha, lambda and gamma variants (**Fig. 5**). In contrast, antibodies produced by mice immunized  
202 with RBD+Alum could neutralize the wild-type SARS-CoV-2 and alpha variant but showed  
203 significantly lower neutralizing activity against gamma and lambda variants (**Fig. 5**). AddaVax and  
204 AddaS03 adjuvanted formulations induced similar neutralizing antibody titers against the wild-type,  
205 gamma and lambda variants (**Fig. 5**).

206 Altogether these results demonstrate that addition of U-Omp19 to the Alum plus RBD  
207 vaccine formulation increases virus neutralizing antibodies, specific IgA in BAL and neutralizing  
208 antibodies of the virus in BAL. Neutralizing antibodies are proposed as the best correlate of  
209 protection thus we focused the next studies on the vaccine formulation containing U-Omp19 as  
210 adjuvant.

### 211 ***U-Omp19+RBD+Alum formulation induces Ag-specific Th1 and CD8<sup>+</sup> T cells in spleen and*** 212 ***lung***

213 In addition to memory B cells and neutralizing antibodies, induction of specific T cell immune  
214 responses could have a role in protection against SARS-CoV-2 infection<sup>27</sup>.

215 To determine T cell-mediated immune responses, splenocytes and lung cells from  
216 RBD+Alum or RBD+Alum+U-Omp19 immunized mice were stimulated with RBD or medium alone  
217 and then cytokines levels in the supernatants were measured. Both formulations were able to  
218 induce Ag-specific cytokine secretion at spleen (**Fig. 6A**). Importantly, the levels of interferon (IFN)- $\gamma$

219 were higher than interleukin (IL)-5 at spleens of both vaccine formulations. In lungs, immunization  
220 with RBD+Alum+U-Omp19 promoted a significant increment in IFN- $\gamma$  secretion compared with the  
221 formulation containing RBD+Alum (**Fig. 6B**). However, the Alum-adjuvanted vaccine elicited a  
222 higher amount of IL-5 by lung (**Fig. 6B**). These results suggest that U-Omp19 as adjuvant promotes  
223 a specific T cell response biased to a Th1 profile in the lung.

224 To further evaluate the Th1/2 balance, IFN- $\gamma$  and IL-4 producing cells were measured by  
225 intracellular cytokine staining. Spleen cells from immunized mice were stimulated with a pool of  
226 SARS-CoV-2 RBD peptides to detect antigen-specific T cell responses. Percentages of IFN- $\gamma$ -  
227 producing CD4<sup>+</sup> and CD8<sup>+</sup> T cells were increased in both groups of mice while IL-4-producing CD4<sup>+</sup>  
228 T cells were only increased after RBD+Alum administration (**Fig. 6C and D**). These results support  
229 the induction of Th1 and CD8<sup>+</sup> T cell immune responses after immunization with RBD adjuvanted  
230 with U-Omp19 in combination with Alum.

### 231 ***U-Omp19 as adjuvant increases neutralizing antibodies in C57BL/6 mice***

232 Immunogenicity of vaccine formulations using Alum alone or combining both adjuvants  
233 (alum and U-Omp19) with RBD as Ag was also evaluated in the C57BL/6 mouse strain. Vaccine  
234 formulations were administered following the same schedule used for BALB/c mice, two doses  
235 every 14 days.

236 Both vaccine formulations induced high anti-RBD IgG titers in sera (**Fig. 7A**). Remarkably,  
237 anti-RBD IgA levels in the BAL of RBD+Alum+U-Omp19 immunized mice were higher than in the  
238 RBD+Alum immunized mice (**Fig. 7B**, \* $p < 0.05$ ). There were no differences in specific IgG levels in  
239 the BAL between both groups (**Fig. 7B**).

240 Formulation containing RBD+U-Omp19+Alum induced higher neutralizing antibody titers  
241 than RBD+Alum formulation (**Fig. 7C**, GMT at 42 days post prime dose: 93.60 95%CI 59.99-452.5  
242 and 37.47 95%CI 23.40-19.36 respectively).

243 Addition of U-Omp19 to RBD plus Alum vaccine increased the neutralizing antibody titers  
244 against authentic wild-type virus. Four weeks after second dose, sera of mice immunized with

245 RBD+Alum+U-Omp19 produced a ten-fold increase in the viral neutralizing antibodies titer (GMT  
246 929 95%CI 37.50-10079 **Fig. 7D**) compared with mice receiving RBD + Alum (**Fig. 7D**, GMT 99  
247 95%CI 13.61-210.1). These results validated the data obtained in BALB/c mice and further indicate  
248 that U-Omp19 can be used under different genetic backgrounds.

249 ***U-Omp19 adjuvanted vaccine increases RBD specific germinal centers cells and***  
250 ***plasmablasts in the spleen***

251 A persistent germinal center (GC) B cell response enables the generation of robust humoral  
252 immunity<sup>28</sup>. Therefore, specific GC B cells were evaluated in spleens from vaccinated mice one  
253 month after second dose, **Fig. 8A** shows the gating strategy used. There were no differences  
254 between groups in the total CG cells (B220<sup>+</sup> CD19<sup>+</sup> IgD<sup>-</sup> CD95<sup>+</sup> GL7<sup>+</sup> cells) among spleen samples  
255 (**Fig. 8B**). Of note, there were differences in the frequency of RBD<sup>+</sup> specific GC cells as mice  
256 immunized with RBD+Alum+U-Omp19 increased the percentage of RBD<sup>+</sup> specific GC cells in  
257 comparison with RBD+Alum (**Fig. 8C**). Besides, the percentages of RBD<sup>+</sup> specific plasma blasts  
258 (B220<sup>+</sup> CD19<sup>+</sup> IgD<sup>-</sup> CD138<sup>+</sup> cells) were also higher in animals from RBD+Alum+U-Omp19 than from  
259 RBD+Alum (**Fig. 8D**). These results indicate a better performance of the vaccine formulation  
260 containing U-Omp19 to induce specific GC and secretory B cells one month after immunization.

261 ***RBD+Alum+U-Omp19 induces protection against intranasal SARS-CoV-2 challenge***

262 To determine vaccine efficacy, we used a severe disease model using K-18-hACE2  
263 transgenic mice. Infection of transgenic mice with SARS-CoV-2 results in lung disease with signs of  
264 diffuse alveolar damage, and variable spread to the central nervous system<sup>29</sup>. The lethal dose 50%  
265 (LD50), is estimated to be 10<sup>4</sup> plaque-forming units (PFU)<sup>30</sup>. Vaccine formulation efficacy was  
266 evaluated in K18-hACE2 mice vaccinated with RBD+Alum+U-Omp19 or PBS (control) and  
267 challenged intranasally with 2x10<sup>5</sup> PFU of SARS-CoV-2. At day 5 post infection some animals were  
268 euthanized to assess the viral load in lungs and brains. The presence of the SARS-CoV-2 virus was  
269 not detected in the lungs while very low virus titers were detected in the brains of animals  
270 vaccinated with RBD+Alum+U-Omp19 (**Fig. 9A**). In contrast a high viral load was detected in the  
271 lungs and brains of animals immunized with PBS (**Fig. 9A**). It is noteworthy that the majority of the

272 mice vaccinated with RBD+Alum+U-Omp19 did not lose weight after challenge (**Fig. 9B**). Thus, the  
273 RBD+Alum+U-Omp19 vaccine induced protection against the experimental challenge with SARS-  
274 CoV-2.

## 275 **Discussion**

276           There is an urgent need to develop safe, effective, and affordable COVID-19 vaccines for  
277 low- and middle-income countries. Such vaccines should rely on proven technologies such as  
278 recombinant protein–based vaccines to facilitate their transfer to emerging market vaccine  
279 manufacturers. Protein-based vaccines are classic vaccine platforms and are considered a very  
280 safe vaccine strategy. The majority of anti-viral vaccines being licensed for human use are protein-  
281 based vaccines, such as hepatitis B and human papillomavirus subunit vaccines, which have been  
282 widely administered, and present an exceptional safety profile<sup>31</sup>.

283           Our group has been working on the development of a recombinant protein–based vaccine to  
284 prevent COVID-19. We selected the SARS-CoV-2 spike protein RBD as an immunogen since it  
285 offers advantages for rational vaccine design both immunologically and from a manufacturability  
286 point of view<sup>32</sup>. RBD targeted binding antibodies correlate very strongly with virus-neutralizing  
287 activity in natural infections and vaccinations<sup>33</sup>. Therefore, selection of RBD as antigen may induce  
288 a higher proportion of neutralizing antibodies, compared to full length Spike protein immunization.  
289 Indeed, B cell repertoire analysis after RBD immunization has been shown to induce a higher  
290 proportion of neutralizing antibodies than full length Spike protein immunization<sup>34</sup>. Moreover, RBD  
291 binding antibodies account for more than 90% of the neutralizing activity in COVID-19 convalescent  
292 sera and vaccinated individuals<sup>33,35</sup>. Previous studies have found that both SARS-CoV and MERS-  
293 CoV display antibody-dependent enhancement (ADE)<sup>36</sup>, where non-neutralizing antibodies  
294 produced in response to a vaccine mediate virus infection via the fragment crystallizable (Fc)  
295 receptor and thus increase the risk of vaccinations enhancing viral infection<sup>37</sup>. Although ADE has  
296 not been reported for the existing COVID-19 vaccines, a recent study has shown that antibodies  
297 against the S protein N-terminal domain enhanced the binding capacity of S protein to ACE2 and  
298 infectivity of SARS-CoV-2<sup>38</sup>. To mitigate the ADE effect, minimizing non-neutralizing epitopes we  
299 decided to work with the SARS-CoV-2 spike protein RBD. Furthermore, in our hands (data not  
300 shown) and as described by others<sup>39</sup>, yields of recombinant RBD were much higher than those of  
301 full-length Spike, an important factor in delivering the vaccine to global population.

302 Different cell types have been used to produce RBD antigens, such as yeast, plant and  
303 insect cells<sup>32,40-43</sup>. However, production in mammalian cells<sup>11,44-48</sup> may produce a RBD antigenic  
304 domain that more closely resembles that generated during virus infection in human cells (including  
305 post-translational modifications such as glycosylation and correct folding)<sup>49</sup>. Our results showing  
306 binding to hACE2 expressing cells and the induction of neutralizing antibody titers confirm the  
307 preservation of the RBD structure and the suitable exposition of the receptor binding motif (RBM).

308 In this work we have assessed the immunogenicity in mice of four different formulations  
309 containing the SARS-CoV-2 spike protein RBD with: i) human approved vaccine adjuvants:  
310 Alhydrogel (Alum), an  $\alpha$ -tocopherol and squalene-based containing oil-in-water emulsion (AddaS03)  
311 or a squalene-based oil-in-water nano-emulsion (AddaVax) or ii) a combination of Alum and a novel  
312 adjuvant called U-Omp19, a bacterial protease inhibitor with adjuvant properties. All adjuvanted  
313 formulations induced robust anti-SARS-CoV-2 antibody responses. However, only alum containing  
314 formulations resulted in detectable antibody titers after the first immunization. This result is in line  
315 with literature reporting low immunogenicity in mice after a single dose when RBD is formulated with  
316 AddaVax<sup>50-53</sup>, but significant seroconversion titers after single dose when formulated with alum<sup>40,53</sup>  
317 or after two doses when formulated with AddaVax or AddaS03<sup>39,46,50,51,53</sup>. The overall response was  
318 dominated by the IgG1 subclass in all immunized groups. Interestingly, in COVID-19 recovered  
319 individuals spike specific IgG1 antibodies correlated most closely with *in vitro* viral neutralization  
320 than other IgG subclasses<sup>54</sup>.

321 RBD-immunization with Alum, AddaS03, AddaVax or U-Omp19 + Alum induced substantial  
322 neutralizing antibody titers against Spike-pseudotyped virions and wild-type SARS-CoV-2. Notably,  
323 the formulation adjuvanted with Alum + U-Omp19 induced stronger neutralizing antibody titers when  
324 compared to formulations adjuvanted with Alum, AddaVax or AddaS03. A similar effect of U-Omp19  
325 in antibody functionality was seen with recombinant subunit vaccine against *Trypanosoma cruzi*,  
326 where a formulation adjuvanted with U-Omp19 despite inducing lower antibody titers, showed  
327 strong antibody mediated lytic activity, which together with the induction of a Th1-biased immune  
328 response may account for the better elicited protection of this formulation<sup>21</sup>. This improvement in

329 antibody function by U-Omp19 addition to formulations could also be due to its protease inhibitor  
330 activity. U-Omp19 can inhibit neutrophil elastase<sup>18</sup> and Kim et al. have recently shown that  
331 coadministration of a neutrophil elastase inhibitor enhances the affinity and function of antibodies  
332 induced by alum as adjuvant<sup>55</sup>. In the same work, Kim et al. showed that neutrophil elastase  
333 inhibitor supplementation can improve the efficacy of alum-adsorbed anti-SARS-CoV-2 vaccines by  
334 promoting the induction of IgA in the serum and mucosal secretions<sup>55</sup>. Of note, U-Omp19  
335 adjuvanted group presented the highest levels of RBD specific IgA in serum and BAL and the  
336 highest neutralizing activity against SARS-CoV-2 Spike-pseudotyped virions in BAL. This local  
337 immune response in the lungs may be of vital importance in neutralizing the virus before infection  
338 establishment, since it has been suggested that IgA-mediated mucosal immunity may be a critical  
339 defense mechanism against SARS-CoV-2 that may reduce infectivity of human secretions and  
340 consequently viral transmission as well<sup>24</sup>. Moreover, secretory dimeric IgA found in mucosa has  
341 been shown to be a more potent SARS-CoV-2 neutralizer than serum IgA<sup>56</sup>.

342         Recently, new variants of concern (VOC) or interest (VOI) of SARS-CoV-2 have been  
343 identified worldwide, and many of them have been shown to partially escape neutralization by  
344 antibodies induced by infection with previous circulating variants or vaccines<sup>25,26</sup>. These variants  
345 harbor mutations in RBD and N-terminal domain (NTD) of the spike protein that could impair the  
346 neutralizing activity of vaccine-induced antibodies<sup>4</sup>. Therefore, we also evaluated the neutralizing  
347 activity induced by the vaccine formulations against highly circulating SARS-CoV-2 variants in our  
348 region: alpha (B.1.1.7), gamma (P1), and Lambda (C.37). Neutralizing activity of antibodies elicited  
349 by the vaccine formulation with alum alone was 2-fold lower for Gamma and Lambda SARS-CoV-2  
350 variants compared to ancestral (D614G) and alpha SARS-CoV-2 variants, similar or higher variant  
351 escape to vaccine induced neutralizing antibodies was described for several vaccines<sup>39,57,58</sup>.  
352 Interestingly the AddaVax and AddaS03 adjuvanted formulations induced similar neutralizing  
353 antibody titers against the wild-type, gamma and lambda variants. These results are in line with  
354 published data for CHO cell expressed RBD formulated with AddaS03<sup>39</sup>. More importantly, RBD  
355 adjuvanted with U-Omp19 + Alum induced significantly higher and broader neutralizing activity.

356 These data agree with other works showing that adjuvants not only enhance immunogenicity, but  
357 also may have different potential to elicit neutralizing antibodies that provide a greater breadth of  
358 neutralization<sup>59</sup>.

359 Most effective vaccines generate prolonged immunity by eliciting long-lived plasma cells  
360 (LLPCs) and memory B cells (MBCs)<sup>60</sup>. LLPCs and MBCs with high affinity for the antigen are  
361 formed during germinal center reactions. In this study we have shown that RBD immunization with  
362 Alum+U-Omp19 induced higher levels of RBD specific GC B cells than RBD formulated with alum  
363 alone. It has been reported that RBD specific GC responses strongly correlate with neutralizing  
364 antibody production<sup>61</sup>. It has also been suggested that prolonged antigen availability along with  
365 continuous presentation of antigens via major histocompatibility complex class II can improve GC  
366 reactions<sup>61</sup>. We have previously demonstrated that U-Omp19 increases antigen half-life in antigen  
367 presenting cells<sup>19,62</sup>, and thus may increase GC reactions and CD4<sup>+</sup> T cell activation. Also, it has  
368 been shown that neutrophil elastase inhibitor supplementation to alum formulations increases the  
369 frequency of GC B cells and the size of GC<sup>55</sup>, suggesting that enrichment of RBD-specific GC B  
370 cells induced by U-Omp19 could be related to its ability to inhibit neutrophil elastase. U-Omp19  
371 ability to increase GC B cell reactions was also demonstrated in the context of a rabies vaccine, in  
372 which the addition of U-Omp19 resulted in enhanced immunogenicity through increasing dendritic  
373 cells activation and germinal center formation<sup>63</sup>.

374 Although antibodies have been shown to play a critical role in protection against coronavirus  
375 infections, the T cell response is still indispensable for virus clearance, decreasing severe illness,  
376 and prognostic recovery<sup>64</sup>. A study by McMahan et. al. in rhesus macaques suggested that vaccine  
377 induced memory T-cell responses contribute to protection against SARS-CoV-2, especially when  
378 antibodies work sub-optimally<sup>14</sup>. In this study, we have investigated the intensity and diversity of T  
379 cells elicited in the lungs and the spleens in response to vaccination with RBD formulated with Alum  
380 or with Alum + U-Omp19. Interestingly, immunization with RBD adjuvanted with Alum alone induced  
381 a Th2 biased response in the lungs and a Th1/Th2 profile in the spleens, the addition of U-Omp19  
382 biased the response to a Th1 profile, with predominance of IFN- $\gamma$  production in the lung. Both



383 vaccine formulations induced both IFN- $\gamma$ <sup>+</sup> CD4<sup>+</sup> as well as IFN- $\gamma$ <sup>+</sup> CD8<sup>+</sup> T cell responses, while IL-4<sup>+</sup>  
384 CD4<sup>+</sup> were induced only after immunization with RBD + Alum. Similar results have been reported for  
385 a formulation containing RBD and Alum that induced a mixed Th1/Th2 immune response<sup>40</sup>.  
386 Interestingly, an RBD dimer vaccine formulated with AddaVax was unable to elicit a T cell response  
387 in the mouse model<sup>65</sup>. Our results highlight that Th1 or Th2 responses are mainly dependent on the  
388 type of adjuvant. Notably, SARS-CoV-2 enhanced immunopathology was associated with Th2-  
389 biased responses<sup>66</sup>. Therefore, the addition of U-Omp19 may be a way to prevent immunopathology  
390 during SARS-CoV-2 infection in vaccinated individuals.

391 Importantly, the *in vivo* functionality of RBD+Alum+U-Omp19 vaccine elicited immune  
392 responses was evaluated in a severe disease COVID19 murine model showing that this vaccine  
393 was able to confer protection in lungs and brains from i.n. SARS-CoV-2 challenged K18-hACE2  
394 mice.

395 Vaccine formulation presented in this study can be further updated against new SARS-CoV-  
396 2 variants and be used as primary immunization and also as heterologous booster for other  
397 vaccines. Interestingly, priming with full-length Spike and then boosting with SARS-CoV-2 RBD  
398 'immuno-focuses' neutralizing antibody responses to the RBD protein in mice and macaques<sup>50</sup> and  
399 might represent an approach to redirect immunity against SARS-CoV-2 variants.

400 While RBD+Alum induces significant immune responses, it has been suggested that its  
401 immunogenicity should be increased. Different approaches have been proposed to increase its  
402 immunogenicity, such as i) expression as dimer<sup>42,48,65,67</sup> or trimers<sup>44</sup>, ii) fusion to carrier proteins like  
403 human IgG Fc moiety<sup>43,67</sup>, tetanus toxoid<sup>11</sup>, interferon- $\alpha$ <sup>67</sup>, iii) addition of pan HLA-DR-binding  
404 epitope to enhance helper T cell responses<sup>67</sup>, iv) using nanoparticles as delivery system<sup>41,45,47,52,59</sup>  
405 or v) addition of immunopotentiators as CpG<sup>41,42,46,59</sup>, MPLA<sup>43</sup>, 3M-052 or a TLR-7/8 agonist<sup>44,59</sup>.  
406 Here we demonstrated that the addition of U-Omp19 to RBD + Alum formulation was able to  
407 increase the induction and breadth of SARS-CoV-2 neutralizing antibody responses, increase the  
408 frequency of RBD specific germinal center B cells and induce antigen specific Th1 and CD8<sup>+</sup> T cells.

409 Together our results highlight that the addition of U-Omp19 could be another approach to improve  
410 vaccine formulations comprising an antigen and alum.

## 411 **Materials and Methods**

### 412 **Antigen expression and purification**

413 Codon optimized RBD containing spike signal peptide (residues 1-14) fused to the RBD domain  
414 (residues 319-541) and a C-terminal 6xHis tag was obtained. The protein was expressed from a  
415 pcDNA 3.1 plasmid in HEK 293 cells. Cells grown in monolayer were transfected with  
416 polyethylenimine (PEI) and three days after transfection the supernatant was harvested and clarified  
417 by centrifugation at 1500 x g for 15 min. The recombinant proteins were purified from supernatants  
418 by affinity chromatography with a Ni-agarose column (HisTrap™ HP, GE Healthcare, Chicago, IL),  
419 dialyzed against PBS, quantified, and stored at -80°C. LPS contamination from RBD was adsorbed  
420 with Sepharose–polymyxin B (Sigma Aldrich. St Louis, MO). Endotoxin determination was  
421 performed with a Limulus amoebocyte chromogenic assay (Lonza, Basel.).

### 422 **SDS-PAGE and western blot analysis**

423 RBD samples were run under reducing conditions by SDS-PAGE. Samples were mixed with  
424 Laemmli sample buffer with  $\beta$ -Mercaptoethanol. The samples were incubated at 95 °C for 5 min.  
425 Protein bands were visualized by staining with Coomassie blue R250. Bands were then transferred  
426 to a nitrocellulose membrane (GE, Healthcare. Chicago, IL), blocked with tris buffered saline (TBS)-  
427 Tween 0.05%, and incubated with human convalescent serum (1/100 dilution). An anti-human  
428 IRDye 800 (1/2000 dilution) was used as a secondary antibody for Infrared fluorescence detection  
429 on the Odyssey Imaging System.

### 430 **Size exclusion chromatography analysis of the Spike RBD domain.**

431 SEC runs were performed on a Superdex 75 column by injecting 150  $\mu$ g of RBD protein in 20mM  
432 Sodium phosphate buffer, pH 7.0 and 0.2M NaCl in the absence of DTT. Runs were performed at a  
433 flow rate of 0.4 ml/min. Apparent molecular weight was calculated by calibrating the column with

434 molecular weight markers: Bovine Serum Albumin (66.4 KDa), Ovalbumin (44.3 KDa), Papain (23  
435 KDa) Ribonuclease A (13.7 KDa) and Aprotinin (6.5 KDa) with  $V_o = 8.1\text{ml}$  and  $V_o+V_i = 19.5\text{ml}$ .

#### 436 **Adjuvants and vaccine formulations**

437 Recombinant U-Omp19 was expressed in *E. coli* cells and purified as previously described in<sup>17</sup>. LPS  
438 contamination from RBD was adsorbed with sepharose–polymyxin B (Sigma Aldrich. St Louis, MO).  
439 Endotoxin determination was performed with a Limulus ameocyte chromogenic assay (Lonza,  
440 Basel). U-Omp19 preparations used contained <0.1 endotoxin units per milligram protein.

441 AddaVax or AddaS03 were purchased at Invivogen and Alhydrogel 2% was kindly provided by  
442 CRODA. In vaccine formulations Ag and U-Omp19 were absorbed to Alhydrogel. RBD and U-  
443 Omp19 proteins were adsorbed to Alhydrogel® (CRODA, Inc.). Protein adsorption was analyzed by  
444 sodium dodecyl sulfate-polyacrylamide gel electrophoresis, followed by Coomassie staining. Protein  
445 concentration was determined by the bicinchoninic acid method.

#### 446 **Ethics statement**

447 All experimental protocols with animals were conducted in strict accordance with international  
448 ethical standards for animal experimentation (Helsinki Declaration and its amendments, Amsterdam  
449 Protocol of welfare and animal protection and National Institutes of Health, USA NIH, guidelines).  
450 The protocols performed were also approved by the Institutional Committee for the use and care of  
451 experimental animals (CICUAE) from National University of San Martin (UNSAM) (01/2020).

#### 452 **Animals and immunizations**

453 Eight-week-old female BALB/c or C57BL/6 mice were obtained from IIB UNSAM animal facility.  
454 Animals were intramuscularly (i.m) inoculated at day 0 and 14 with i) RBD + Alhydrogel (n=5), ii)  
455 RBD + Alhydrogel + U-Omp19 (n=5), iii) RBD + AddaVax (n=5) and iv) RBD + AddaS03 (n=4).  
456 Blood samples were collected weekly to measure total and neutralizing antibody titers. At day 42  
457 post prime immunization animals were sacrificed and spleens, lungs and bronchoalveolar lavages  
458 (BAL) were obtained.

#### 459 **Determination of antibody levels in serum and BAL**

460 RBD- specific antibody responses (IgA, IgG, IgG1, IgG2a) were evaluated by indirect ELISA. 96-  
461 well plates were coated with 0.1 µg/well of RBD in phosphate buffered saline (PBS) overnight at 4  
462 °C. Plates were washed with PBS-Tween 0.05% and blocked with PBS-Tween 0.01% 1% non-fat  
463 milk for 1 h. Plates were then incubated with sera or BAL (diluted in PBS Tween 0.01% containing  
464 1% non-fat milk) for 1 h and then plates were washed and incubated with HRP conjugated anti-  
465 mouse IgA, IgG (SIGMA, St. Louis, MO, USA), IgG1 or IgG2a (ThermofisherScientific, Waltham,  
466 MA) for 1 h at 37 °C. Then, TMB (3,3',5,5'-tetramethylbenzidine) was added and reaction was  
467 stopped with H<sub>2</sub>SO<sub>4</sub> 4 N and immediately read at 450 nm to collect end point ELISA data. End-point  
468 cut-off values for serum titer determination were calculated as the mean specific optical density  
469 (OD) plus 3 standard deviations (SD) from sera of saline immunized mice and titers were  
470 established as the reciprocal of the last dilution yielding an OD higher than the cut-off.

#### 471 **Plasmids**

472 Plasmid pCMV14-3X-Flag-SARS-CoV-2 S was a gift from Zhaohui Qian (Addgene plasmid #  
473 145780)<sup>68</sup>, psPAX2 was a gift from Didier Trono (Addgene plasmid # 12260); and pLB-GFP was a  
474 gift from Stephan Kissler (Addgene plasmid # 11619).

#### 475 **Cell lines**

476 Human embryonic kidney cell line 293T expressing the SV40 T-antigen (HEK-293T, ATCC #CRL-  
477 11268) was kindly provided by Cecilia Frecha (Instituto de Medicina Traslacional e Ingeniería  
478 Biomédica, Hospital Italiano de Buenos Aires) and maintained in complete Dulbecco's Modified  
479 Eagle's Medium (DMEM, Gibco) containing 10% (vol/vol) fetal bovine serum (FBS, Internegocios),  
480 100 IU/mL penicillin, and 100 µg/mL streptomycin (Gibco). For lentivirus production, HEK-293T cells  
481 were maintained in DMEM10 containing 100 µg/ml G418 (Sigma Aldrich. St Louis, MO). African  
482 green monkey kidney cell line Vero E6 ATCC #CRL-1586 were cultured at 37°C in 5% CO<sub>2</sub> in  
483 Dulbecco's Modified Eagle's high glucose medium (Sigma Aldrich) supplemented with 5% fetal  
484 bovine serum (FBS) (Sigma Aldrich).

485 HEK-293T cells expressing the SARS-CoV-2 receptor protein ACE2 (HEK-hACE2) were  
486 established in our laboratory by lentivirus transduction. Clonal selection of HEK-hACE2 was  
487 achieved by limit dilution and selection with hygromycin 200 µg/ml.

#### 488 **SARS-CoV-2 Pseudovirus (PsV) production**

489 For SARS-CoV-2 pseudovirus production,  $5 \times 10^6$  HEK-293T cells were seeded in complete DMEM  
490 in 10-cm dishes and incubated 24 h at 37°C and 5% CO<sub>2</sub>. Pseudoviruses were obtained by co-  
491 transfection with psPAX2, pCMV14-3xFlag SARS-CoV-2 S and pLB GFP by using polyetherimide  
492 (PEI) (1:2, DNA:PEI). The supernatants were harvested at 72 h post transfection and centrifuged at  
493 3000 × g for 15 min at 4°C. HEPES was added then to a final concentration of 20 mM to the  
494 supernatant, which was then passed through 0.45 µm filter. When necessary, pseudovirus  
495 suspensions were concentrated by an overnight centrifugation at 3000 x g at 4 °C. PVS was titrated  
496 in HEK-hACE2 cells and stored at -70°C until use.

#### 497 **Pseudovirus neutralization assay (PsVNA)**

498 HEK-hACE2 cells were seeded in 96-well plates in DMEM10 and incubated 24h at 37°C and 5%  
499 CO<sub>2</sub>. SARS-CoV-2 PsV (500-800 focus-forming units, FFU) were preincubated with serially diluted  
500 sera for 1h at 37°C. Then, PsV-sera mixture was added to HEK-hACE2 and centrifuged at 2500 rpm  
501 for 1h at 26°C. After a 72h incubation at 37°C and 5% CO<sub>2</sub>, cultures were fixed with 4%  
502 paraformaldehyde for 20 min. Transduced cells express GFP, and neutralization titer 50 (NT50) was  
503 defined as the reciprocal serum dilution that causes a 50% reduction of transduction efficiency.

#### 504 **Viruses**

505 SARS-CoV-2 reference strain (hCoV-19/Argentina/PAIS-G0001/2020 GISAID Accession ID:  
506 EPI\_ISL\_499083) was obtained from Dr. Sandra Gallegos (InViV working group). SARS-CoV-2  
507 Gamma P.1 (GISAID Accession ID: EPI\_ISL\_2756556) and alpha (GISAID Accession ID:  
508 EPI\_ISL\_2756558) were isolated in Instituto de Investigaciones Biomédicas en Retrovirus y SIDA  
509 (INBIRS, UBA-CONICET) from nasopharyngeal swabs of patients. SARS-CoV-2 Lambda C.37  
510 (hCoV-19/Argentina/PAIS-A0612/2021 GISAID Accession ID: EPI\_ISL\_3320903) was isolated at

511 INBIRS from a sample of nasopharyngeal swabs kindly transferred by Dr. Viegas and Proyecto  
512 PAIS. Virus was amplified in Vero E6 cells, and each stock was fully sequenced. Studies using  
513 SARS-CoV-2 were done in a Biosafety level 3 laboratory and the protocol was approved by the  
514 INBIRS Institutional Biosafety Committee.

#### 515 **SARS-CoV-2 neutralization assay**

516 Serum samples were heat-inactivated at 56°C for 30 min. Serial dilutions were performed and then  
517 incubated for 1 h at 37°C in the presence of SARS-CoV-2 in DMEM 2% FBS. Fifty µl of the mixtures  
518 were then added to Vero cells monolayers for an hour at 37°C (MOI=0.004). Infectious media was  
519 removed and replaced for DMEM 2% FBS. After 72 h, cells were fixed with PFA 4% (4°C 20 min)  
520 and stained with crystal violet solution in methanol. The cytopathic effect (CPE) of the virus on the  
521 cell monolayer was assessed visually, if even a minor damage to the monolayer (1-2 «plaques»)  
522 was observed in the well, this well was considered as a well with a manifestation of CPE.  
523 Neutralization titer was defined as the highest serum dilution without any CPE in two of three  
524 replicable wells. Otherwise, plates were scanned for determination of media absorbance at 585 nm  
525 and non-linear curves were fitted to obtain the titer corresponding to the 50% of neutralization  
526 (NT50). Neutralization assays to compare neutralization among different SARS-CoV-2 variants  
527 (alpha, gamma and lambda) were performed in the same plate for each sample.

#### 528 **Determination of T cell immune responses**

529 Four weeks after the second dose, mice were sacrificed to study cellular responses. Intracellular  
530 cytokine determination: splenocytes were cultured ( $4 \times 10^6$  cells/well) in the presence of stimulus  
531 medium (complete medium supplemented with anti-CD28 and anti-CD49d) or Ag stimuli (stimulus  
532 medium + RBD-peptides + RBD protein) for 18 h. Next, brefeldin A was added for 5 h to the  
533 samples. After that, cells were washed, fixed, permeabilized, stained, and analyzed by flow  
534 cytometry. The cells were stained with Viability dye (Zombie Aqua), anti-mouse-CD8a Alexa Fluor  
535 488, anti-mouse-CD4 Alexa Fluor 647, anti-IL-4 Brilliant Violet 421 and anti-IFN-γ PE (Biolegend,  
536 San Diego, CA).

537 **Determination of Ag specific B cells.**

538 Ag-specific B cells (plasmablasts and germinal center B cells) present in the spleens were  
539 determined by flow cytometry. Splenocytes were plated ( $2 \times 10^6$  cells/well) and stained with Viability  
540 dye (Zombie Aqua), anti-B220 Alexa Fluor 594, anti-CD19 APC/Cy7, anti-CD138 Brilliant Violet  
541 785, anti-IgD Brilliant Violet 605, anti-GL7 Alexa Fluor 488 and anti-CD95 PE (Biolegend, San  
542 Diego, CA). For Ag-specific detection, cells were also stained with RBD Alexa Fluor 64. Next, cells  
543 were washed, fixed and analyzed by flow cytometry.

544 **Vaccine efficacy in K18-hACE2 mice**

545 Four-week-old K18-hACE2 mice (n=7-8 per group) from Jackson Laboratory were used for  
546 evaluating vaccine efficacy. Mice were separated into two groups: i) control (n=7) PBS immunized  
547 and RBD+Alum+U-Omp19 immunized (n=8). Mice in each group included males and females. They  
548 were i.m immunized at day 0 and 14 as described for immune assays. Four weeks post second  
549 vaccination, mice were challenged intranasally (i.n.) with  $10^5$  PFU of SARS-CoV-2 strain WA1/2010  
550 in each nare. Then, they were monitored daily for weight loss and signs of disease for two weeks  
551 post-challenge. Three mice per group were euthanized at day 5 post-challenge to evaluate organ  
552 viral loads, by plaque assay on Vero E6 cells.

553 **Statistical analysis**

554 Statistical analysis and plotting were performed using GraphPad Prism 8 software (GraphPad  
555 Software, San Diego, CA). In experiments with more than two groups, data were analyzed using  
556 one-way ANOVA with a Bonferroni post-test. When necessary, a logarithmic transformation was  
557 applied prior to the analysis to obtain data with a normal distribution. In experiments with two  
558 groups, an unpaired t test or Mann-Whitney U test were used. A p value  $<0.05$  was considered  
559 significant. When bars were plotted, results were expressed as means  $\pm$  SEM for each group.

560 **Data availability**

561 The authors declare that the data supporting the findings of this study are available from the  
562 corresponding author upon reasonable request.

563 **Acknowledgements**

564 This work was supported by grants from Agencia Nacional de Promoción de la Investigación, el  
565 Desarrollo Tecnológico y la Innovación (AGENCIA I+D+i) and Ministerio de Ciencia, Tecnología e  
566 Innovación (IP COVID-260 and FONARSEC 0001); the Bill and Melinda Gates Foundation through  
567 the Grand Challenges Explorations Initiative (OPP1119024) to J.C. and from National Institute of  
568 Allergy and Infectious Diseases of the National Institutes of Health under Award Number  
569 R01AI153433 to A.J.A.

570 The authors thank to the staff at the Instituto de Investigaciones Biotecnológicas and the Animal  
571 Facility of Universidad de San Martín who facilitate animal studies in this work. The authors would  
572 also like to thank Danielle Porier, Krisangel López, and Manette Tanelus for technical assistance  
573 with the SARS-CoV-2 challenge studies.

574 **Contributions**

575 J.C. and K.A.P. were responsible for overall experimental design and supervision of studies. D.E.A.  
576 constructed and expressed the RBD protein, designed and supervised neutralization studies. L.M.C.  
577 designed and conducted experiments, collected data and performed data analysis. L.M.S, L.A.B  
578 and M.L.D purified RBD, formulated vaccine and conducted experiments. E.F.C. performed  
579 pseudovirus neutralization studies and data analysis. C.P.C. conducted humoral and cellular studies  
580 and data analysis. A.J.A. design, supervise and conduct animal challenge studies and data  
581 analysis. W.S. performed animal challenge studies and data analysis. J.A. conducted long-term  
582 humoral response studies. P.S.P, and I.M. performed neutralization studies with wild-type and  
583 SARS-CoV-2 variants. A.V. and M.S. isolated SARS-CoV-2 variants. L.B.C. performed RBD  
584 characterization by size exclusion chromatography. L.M.C, K.A.P. and J.C. wrote the manuscript. All  
585 authors contributed to manuscript editing.

586 **Competing interest**

587 L.M.C., K.A.P. and J.C. are inventors of a patent related to U-Omp19 “Adjuvant for vaccines,  
588 vaccines that comprise it and uses thereof” PCT/ES2010/070667. The owner of this patent is the



589 National Research Council CONICET. The existence of the patent did not have any role in  
590 experimental design, data collection and analysis, decision to publish, or preparation of this  
591 manuscript. The authors have no financial conflicts of interest to declare.

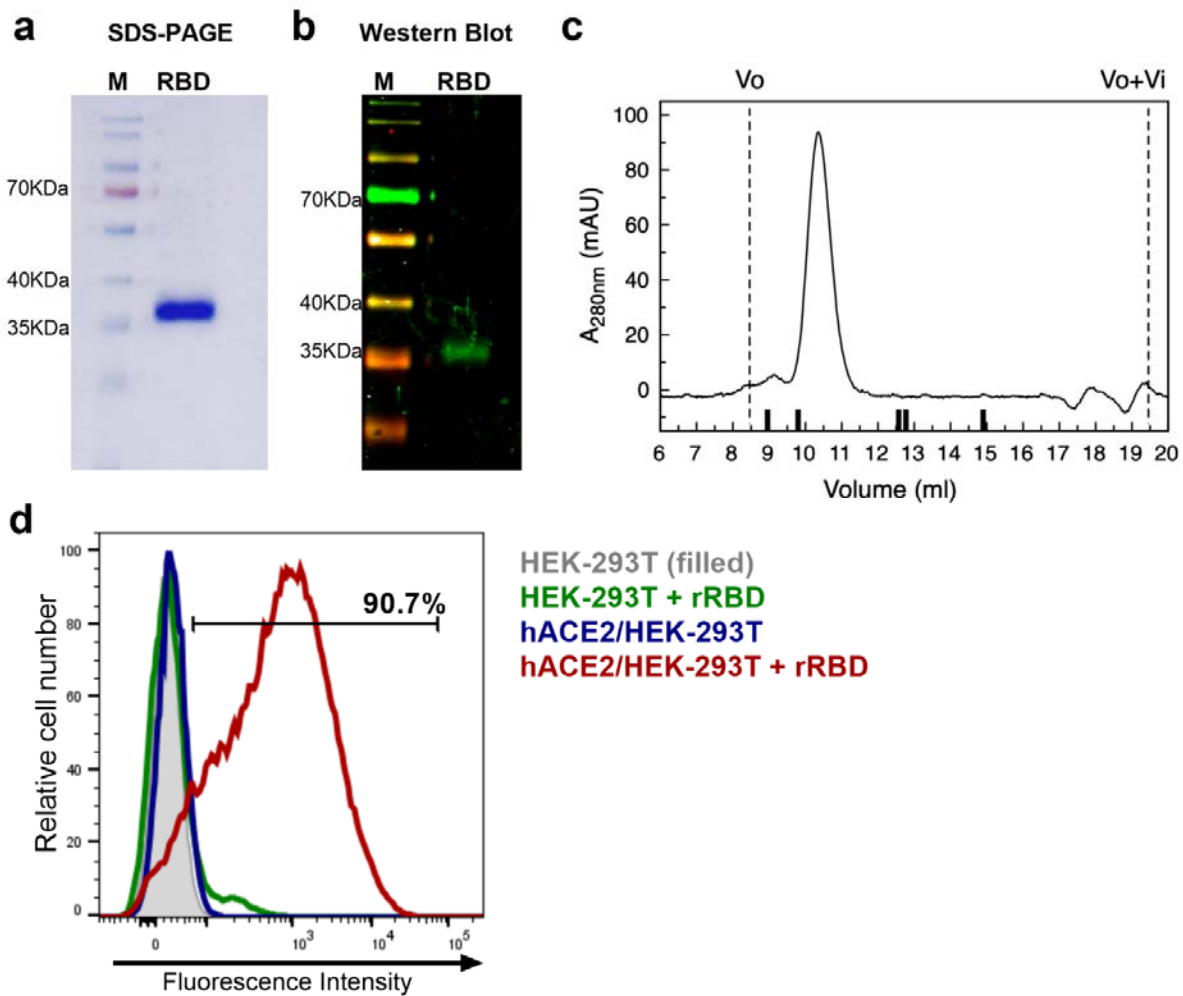
## 592 References

- 593 1 Liu, Y. *et al.* Neutralizing Activity of BNT162b2-Elicited Serum. *New England Journal of Medicine* **384**,  
594 1466-1468, doi:10.1056/nejmc2102017 (2021).
- 595 2 Thomas, S. J. *et al.* Safety and Efficacy of the BNT162b2 mRNA Covid-19 Vaccine through 6 Months.  
596 *New England Journal of Medicine*, doi:10.1056/nejmoa2110345 (2021).
- 597 3 Levin, E. G. *et al.* Waning Immune Humoral Response to BNT162b2 Covid-19 Vaccine over 6  
598 Months. *New England Journal of Medicine*, doi:10.1056/nejmoa2114583 (2021).
- 599 4 Harvey, W. T. *et al.* SARS-CoV-2 variants, spike mutations and immune escape. *Nature Reviews*  
600 *Microbiology* **19**, 409-424, doi:10.1038/s41579-021-00573-0 (2021).
- 601 5 Falsey, A. R. *et al.* SARS-CoV-2 Neutralization with BNT162b2 Vaccine Dose 3. *New England*  
602 *Journal of Medicine*, doi:10.1056/nejmc2113468 (2021).
- 603 6 Mahase, E. Covid-19: Novavax vaccine efficacy is 86% against UK variant and 60% against South  
604 African variant. *BMJ*, n296, doi:10.1136/bmj.n296 (2021).
- 605 7 Letko, M., Marzi, A. & Munster, V. Functional assessment of cell entry and receptor usage for SARS-  
606 CoV-2 and other lineage B betacoronaviruses. *Nat Microbiol* **5**, 562-569, doi:10.1038/s41564-020-  
607 0688-y (2020).
- 608 8 Hoffmann, M. *et al.* SARS-CoV-2 Cell Entry Depends on ACE2 and TMPRSS2 and Is Blocked by a  
609 Clinically Proven Protease Inhibitor. *Cell* **181**, 271-280.e278, doi:10.1016/j.cell.2020.02.052 (2020).
- 610 9 Dai, L. & Gao, G. F. Viral targets for vaccines against COVID-19. *Nature Reviews Immunology* **21**, 73-  
611 82, doi:10.1038/s41577-020-00480-0 (2021).
- 612 10 Jiang, S. *et al.* Roadmap to developing a recombinant coronavirus S protein receptor-binding domain  
613 vaccine for severe acute respiratory syndrome. *Expert Review of Vaccines* **11**, 1405-1413,  
614 doi:10.1586/erv.12.126 (2012).
- 615 11 Valdes-Balbin, Y. *et al.* SARS-CoV-2 RBD-Tetanus Toxoid Conjugate Vaccine Induces a Strong  
616 Neutralizing Immunity in Preclinical Studies. *ACS Chem Biol* **16**, 1223-1233,  
617 doi:10.1021/acscchembio.1c00272 (2021).
- 618 12 Khoury, D. S. *et al.* Neutralizing antibody levels are highly predictive of immune protection from  
619 symptomatic SARS-CoV-2 infection. *Nature Medicine* **27**, 1205-1211, doi:10.1038/s41591-021-  
620 01377-8 (2021).
- 621 13 Earle, K. A. *et al.* Evidence for antibody as a protective correlate for COVID-19 vaccines. *Vaccine* **39**,  
622 4423-4428, doi:10.1016/j.vaccine.2021.05.063 (2021).
- 623 14 McMahan, K. *et al.* Correlates of protection against SARS-CoV-2 in rhesus macaques. *Nature* **590**,  
624 630-634, doi:10.1038/s41586-020-03041-6 (2021).
- 625 15 Wang, H. *et al.* Development of an Inactivated Vaccine Candidate, BBIBP-CorV, with Potent  
626 Protection against SARS-CoV-2. *Cell* **182**, 713-721.e719, doi:10.1016/j.cell.2020.06.008 (2020).
- 627 16 Pulendran, B., S. Arunachalam, P. & O'Hagan, D. T. Emerging concepts in the science of vaccine  
628 adjuvants. *Nature Reviews Drug Discovery* **20**, 454-475, doi:10.1038/s41573-021-00163-y (2021).
- 629 17 Pasquevich, K. A. *et al.* An oral vaccine based on U-Omp19 induces protection against B. abortus  
630 mucosal challenge by inducing an adaptive IL-17 immune response in mice. *PLoS One* **6**, e16203,  
631 doi:10.1371/journal.pone.0016203 (2011).
- 632 18 Ibanez, A. E. *et al.* A bacterial protease inhibitor protects antigens delivered in oral vaccines from  
633 digestion while triggering specific mucosal immune responses. *J Control Release* **220**, 18-28,  
634 doi:10.1016/j.jconrel.2015.10.011 S0168-3659(15)30179-6 [pii] (2015).
- 635 19 Coria, L. M. *et al.* Brucella abortus Omp19 recombinant protein subcutaneously co-delivered with an  
636 antigen enhances antigen-specific T helper 1 memory responses and induces protection against  
637 parasite challenge. *Vaccine* **34**, 430-437, doi:10.1016/j.vaccine.2015.12.012 (2016).
- 638 20 Risso, G. S. *et al.* U-Omp19 from Brucella abortus Is a Useful Adjuvant for Vaccine Formulations  
639 against Salmonella Infection in Mice. *Front Immunol* **8**, 171, doi:10.3389/fimmu.2017.00171 (2017).
- 640 21 Caeiro, L. D. *et al.* The Trypanosoma cruzi TcTASV-C protein subfamily administered with U-Omp19  
641 promotes a protective response against a lethal challenge in mice. *Vaccine* **38**, 7645-7653,  
642 doi:10.1016/j.vaccine.2020.10.006 (2020).

- 643 22 Grifoni, A. *et al.* SARS-CoV-2 human T cell epitopes: Adaptive immune response against COVID-19.  
644 *Cell Host & Microbe* **29**, 1076-1092, doi:10.1016/j.chom.2021.05.010 (2021).
- 645 23 Brito, L. A. & Singh, M. Acceptable levels of endotoxin in vaccine formulations during preclinical  
646 research. *J Pharm Sci* **100**, 34-37, doi:10.1002/jps.22267 (2011).
- 647 24 Sterlin, D. *et al.* IgA dominates the early neutralizing antibody response to SARS-CoV-2. *Sci Transl*  
648 *Med* **13**, doi:10.1126/scitranslmed.abd2223 (2021).
- 649 25 Acevedo, M. L. *et al.* Infectivity and immune escape of the new SARS-CoV-2 variant of interest  
650 *Lambda* (Cold Spring Harbor Laboratory, 2021).
- 651 26 Sabino, E. C. *et al.* Resurgence of COVID-19 in Manaus, Brazil, despite high seroprevalence. *The*  
652 *Lancet* **397**, 452-455, doi:10.1016/s0140-6736(21)00183-5 (2021).
- 653 27 Bange, E. M. *et al.* CD8+ T cells contribute to survival in patients with COVID-19 and hematologic  
654 cancer. *Nature Medicine* **27**, 1280-1289, doi:10.1038/s41591-021-01386-7 (2021).
- 655 28 Turner, J. S. *et al.* SARS-CoV-2 mRNA vaccines induce persistent human germinal centre responses.  
656 *Nature* **596**, 109-113, doi:10.1038/s41586-021-03738-2 (2021).
- 657 29 Winkler, E. S. *et al.* SARS-CoV-2 infection of human ACE2-transgenic mice causes severe lung  
658 inflammation and impaired function. *Nature Immunology* **21**, 1327-1335, doi:10.1038/s41590-020-  
659 0778-2 (2020).
- 660 30 Jiang, R.-D. *et al.* Pathogenesis of SARS-CoV-2 in Transgenic Mice Expressing Human Angiotensin-  
661 Converting Enzyme 2. *Cell* **182**, 50-58.e58, doi:10.1016/j.cell.2020.05.027 (2020).
- 662 31 Kyriakidis, N. C., Lopez-Cortes, A., Gonzalez, E. V., Grimaldos, A. B. & Prado, E. O. SARS-CoV-2  
663 vaccines strategies: a comprehensive review of phase 3 candidates. *NPJ Vaccines* **6**, 28,  
664 doi:10.1038/s41541-021-00292-w (2021).
- 665 32 Hotez, P. J. & Bottazzi, M. E. Developing a low-cost and accessible COVID-19 vaccine for global  
666 health. *PLoS Negl Trop Dis* **14**, e0008548, doi:10.1371/journal.pntd.0008548 (2020).
- 667 33 Piccoli, L. *et al.* Mapping Neutralizing and Immunodominant Sites on the SARS-CoV-2 Spike  
668 Receptor-Binding Domain by Structure-Guided High-Resolution Serology. *Cell* **183**, 1024-1042  
669 e1021, doi:10.1016/j.cell.2020.09.037 (2020).
- 670 34 Tian, S. *et al.* Distinct BCR repertoires elicited by SARS-CoV-2 RBD and S vaccinations in mice. *Cell*  
671 *Discov* **7**, 91, doi:10.1038/s41421-021-00331-9 (2021).
- 672 35 Greaney, A. J. *et al.* Antibodies elicited by mRNA-1273 vaccination bind more broadly to the receptor  
673 binding domain than do those from SARS-CoV-2 infection. *Sci Transl Med* **13**,  
674 doi:10.1126/scitranslmed.abi9915 (2021).
- 675 36 Smatti, M. K., Al Thani, A. A. & Yassine, H. M. Viral-Induced Enhanced Disease Illness. *Front*  
676 *Microbiol* **9**, 2991, doi:10.3389/fmicb.2018.02991 (2018).
- 677 37 Wan, Y. *et al.* Molecular Mechanism for Antibody-Dependent Enhancement of Coronavirus Entry. *J*  
678 *Virology* **94**, doi:10.1128/JVI.02015-19 (2020).
- 679 38 Liu, Y. *et al.* An infectivity-enhancing site on the SARS-CoV-2 spike protein targeted by antibodies.  
680 *Cell* **184**, 3452-3466 e3418, doi:10.1016/j.cell.2021.05.032 (2021).
- 681 39 Law, J. L. M. *et al.* SARS-COV-2 recombinant Receptor-Binding-Domain (RBD) induces neutralizing  
682 antibodies against variant strains of SARS-CoV-2 and SARS-CoV-1. *Vaccine* **39**, 5769-5779,  
683 doi:10.1016/j.vaccine.2021.08.081 (2021).
- 684 40 Yang, J. *et al.* A vaccine targeting the RBD of the S protein of SARS-CoV-2 induces protective  
685 immunity. *Nature* **586**, 572-577, doi:10.1038/s41586-020-2599-8 (2020).
- 686 41 Dalvie, N. C. *et al.* Engineered SARS-CoV-2 receptor binding domain improves manufacturability in  
687 yeast and immunogenicity in mice. *Proc Natl Acad Sci U S A* **118**, doi:10.1073/pnas.2106845118  
688 (2021).
- 689 42 Zang, J. *et al.* Yeast-produced RBD-based recombinant protein vaccines elicit broadly neutralizing  
690 antibodies and durable protective immunity against SARS-CoV-2 infection. *Cell Discov* **7**, 71,  
691 doi:10.1038/s41421-021-00315-9 (2021).
- 692 43 Siriwananon, K. *et al.* Immunogenicity Studies of Plant-Produced SARS-CoV-2 Receptor Binding  
693 Domain-Based Subunit Vaccine Candidate with Different Adjuvant Formulations. *Vaccines (Basel)* **9**,  
694 doi:10.3390/vaccines9070744 (2021).
- 695 44 Routhu, N. K. *et al.* SARS-CoV-2 RBD trimer protein adjuvanted with Alum-3M-052 protects from  
696 SARS-CoV-2 infection and immune pathology in the lung. *Nat Commun* **12**, 3587,  
697 doi:10.1038/s41467-021-23942-y (2021).
- 698 45 Salzer, R. *et al.* Single-dose immunisation with a multimerised SARS-CoV-2 receptor binding domain  
699 (RBD) induces an enhanced and protective response in mice. *FEBS Lett* **595**, 2323-2340,  
700 doi:10.1002/1873-3468.14171 (2021).

- 701 46 Nanishi, E. *et al.* Alum:CpG adjuvant enables SARS-CoV-2 RBD-induced protection in aged mice and  
702 synergistic activation of human elder type 1 immunity. *bioRxiv*, doi:10.1101/2021.05.20.444848  
703 (2021).
- 704 47 Halfmann, P. J. *et al.* Potent neutralization of SARS-CoV-2 including variants of concern by vaccines  
705 presenting the receptor-binding domain multivalently from nanoscaffolds. *Bioeng Transl Med* **6**,  
706 e10253, doi:10.1002/btm2.10253 (2021).
- 707 48 Pan, X. *et al.* RBD-homodimer, a COVID-19 subunit vaccine candidate, elicits immunogenicity and  
708 protection in rodents and nonhuman primates. *Cell Discov* **7**, 82, doi:10.1038/s41421-021-00320-y  
709 (2021).
- 710 49 Starr, T. N. *et al.* Deep Mutational Scanning of SARS-CoV-2 Receptor Binding Domain Reveals  
711 Constraints on Folding and ACE2 Binding. *Cell* **182**, 1295-1310 e1220, doi:10.1016/j.cell.2020.08.012  
712 (2020).
- 713 50 Tan, H. X. *et al.* Immunogenicity of prime-boost protein subunit vaccine strategies against SARS-  
714 CoV-2 in mice and macaques. *Nat Commun* **12**, 1403, doi:10.1038/s41467-021-21665-8 (2021).
- 715 51 Mandolesi, M. *et al.* SARS-CoV-2 protein subunit vaccination of mice and rhesus macaques elicits  
716 potent and durable neutralizing antibody responses. *Cell Rep Med* **2**, 100252,  
717 doi:10.1016/j.xcrm.2021.100252 (2021).
- 718 52 Walls, A. C. *et al.* Elicitation of Potent Neutralizing Antibody Responses by Designed Protein  
719 Nanoparticle Vaccines for SARS-CoV-2. *Cell* **183**, 1367-1382 e1317, doi:10.1016/j.cell.2020.10.043  
720 (2020).
- 721 53 Shrivastava, T. *et al.* Comparative Immunomodulatory Evaluation of the Receptor Binding Domain of  
722 the SARS-CoV-2 Spike Protein; a Potential Vaccine Candidate Which Imparts Potent Humoral and  
723 Th1 Type Immune Response in a Mouse Model. *Front Immunol* **12**, 641447,  
724 doi:10.3389/fimmu.2021.641447 (2021).
- 725 54 Yates, J. L. *et al.* Serological analysis reveals an imbalanced IgG subclass composition associated  
726 with COVID-19 disease severity. *Cell Rep Med* **2**, 100329, doi:10.1016/j.xcrm.2021.100329 (2021).
- 727 55 Kim, E. *et al.* Inhibition of elastase enhances the adjuvanticity of alum and promotes anti-SARS-CoV-  
728 2 systemic and mucosal immunity. *Proc Natl Acad Sci U S A* **118**, doi:10.1073/pnas.2102435118  
729 (2021).
- 730 56 Wang, Z. *et al.* Enhanced SARS-CoV-2 neutralization by dimeric IgA. *Sci Transl Med* **13**,  
731 doi:10.1126/scitranslmed.abf1555 (2021).
- 732 57 Hoffmann, M. *et al.* SARS-CoV-2 variants B.1.351 and P.1 escape from neutralizing antibodies. *Cell*  
733 **184**, 2384-2393 e2312, doi:10.1016/j.cell.2021.03.036 (2021).
- 734 58 Wang, G. L. *et al.* Susceptibility of Circulating SARS-CoV-2 Variants to Neutralization. *N Engl J Med*  
735 **384**, 2354-2356, doi:10.1056/NEJMc2103022 (2021).
- 736 59 Arunachalam, P. S. *et al.* Adjuvanting a subunit COVID-19 vaccine to induce protective immunity.  
737 *Nature* **594**, 253-258, doi:10.1038/s41586-021-03530-2 (2021).
- 738 60 Sallusto, F., Lanzavecchia, A., Araki, K. & Ahmed, R. From vaccines to memory and back. *Immunity*  
739 **33**, 451-463, doi:10.1016/j.immuni.2010.10.008 (2010).
- 740 61 Lederer, K. *et al.* SARS-CoV-2 mRNA Vaccines Foster Potent Antigen-Specific Germinal Center  
741 Responses Associated with Neutralizing Antibody Generation. *Immunity* **53**, 1281-1295 e1285,  
742 doi:10.1016/j.immuni.2020.11.009 (2020).
- 743 62 Coria, L. M. *et al.* A Brucella spp. Protease Inhibitor Limits Antigen Lysosomal Proteolysis, Increases  
744 Cross-Presentation, and Enhances CD8+ T Cell Responses. *J Immunol* **196**, 4014-4029,  
745 doi:10.4049/jimmunol.1501188 (2016).
- 746 63 Zhao, J. *et al.* A novel oral rabies vaccine enhances the immunogenicity through increasing dendritic  
747 cells activation and germinal center formation by expressing U-OMP19 in a mouse model. *Emerg*  
748 *Microbes Infect* **10**, 913-928, doi:10.1080/22221751.2021.1923341 (2021).
- 749 64 Jung, M. K. & Shin, E. C. Phenotypes and Functions of SARS-CoV-2-Reactive T Cells. *Mol Cells* **44**,  
750 401-407, doi:10.14348/molcells.2021.0079 (2021).
- 751 65 Dai, L. *et al.* A Universal Design of Betacoronavirus Vaccines against COVID-19, MERS, and SARS.  
752 *Cell* **182**, 722-733 e711, doi:10.1016/j.cell.2020.06.035 (2020).
- 753 66 Simon, H. U., Karaulov, A. V. & Bachmann, M. F. Strategies to Prevent SARS-CoV-2-Mediated  
754 Eosinophilic Disease in Association with COVID-19 Vaccination and Infection. *Int Arch Allergy*  
755 *Immunol* **181**, 624-628, doi:10.1159/000509368 (2020).
- 756 67 Sun, S. *et al.* Interferon-armed RBD dimer enhances the immunogenicity of RBD for sterilizing  
757 immunity against SARS-CoV-2. *Cell Res* **31**, 1011-1023, doi:10.1038/s41422-021-00531-8 (2021).
- 758 68 Ou, X. *et al.* Characterization of spike glycoprotein of SARS-CoV-2 on virus entry and its immune  
759 cross-reactivity with SARS-CoV. *Nat Commun* **11**, 1620, doi:10.1038/s41467-020-15562-9 (2020).
- 760

761 **Figure 1.**

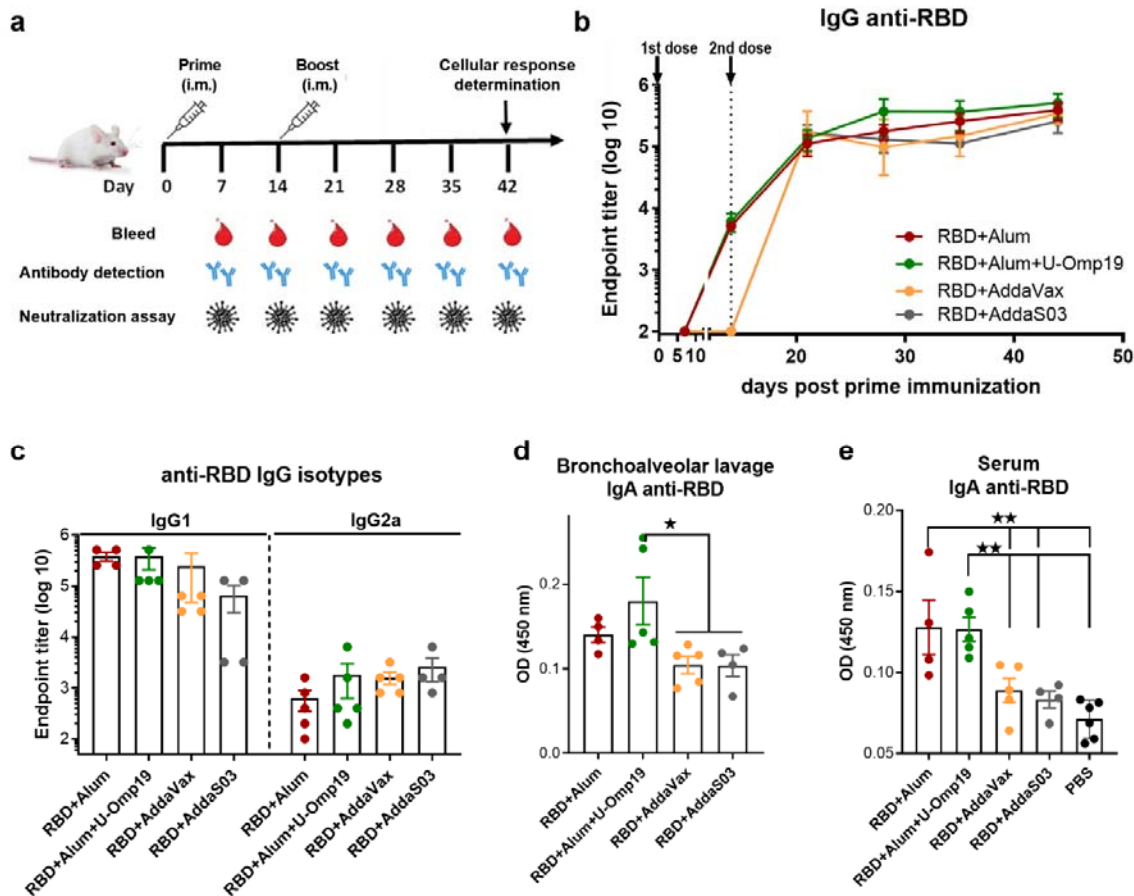


762  
763  
764  
765  
766  
767  
768  
769  
770  
771  
772  
773  
774  
775  
776  
777  
778  
779  
780  
781

**Figure 1. Characterization of recombinant RBD. A.** Coomassie blue- SDS-PAGE stained of reduced RBD. M: page ruler. **B.** Western Blot analysis of recombinant RBD produced in HEK-293 cells using a convalescent human serum as primary antibody. M: page ruler. **C.** Representative size exclusion chromatography elution profile of recombinant RBD. Black bars represent MWM, from left to right: BSA (66.4 KDa), OVA (44.3 KDa), Papain (23 KDa), RNaseA (13.7 KDa), Aprotinin (6.5 KDa), Vo and Vo+Vi are shown as dashed lines. **D.** Binding of recombinant RBD (rRBD) to HEK-293T cells expressing hACE2. HEK-293T were used as control. Histograms and percentage of cells positive for RBD are shown.



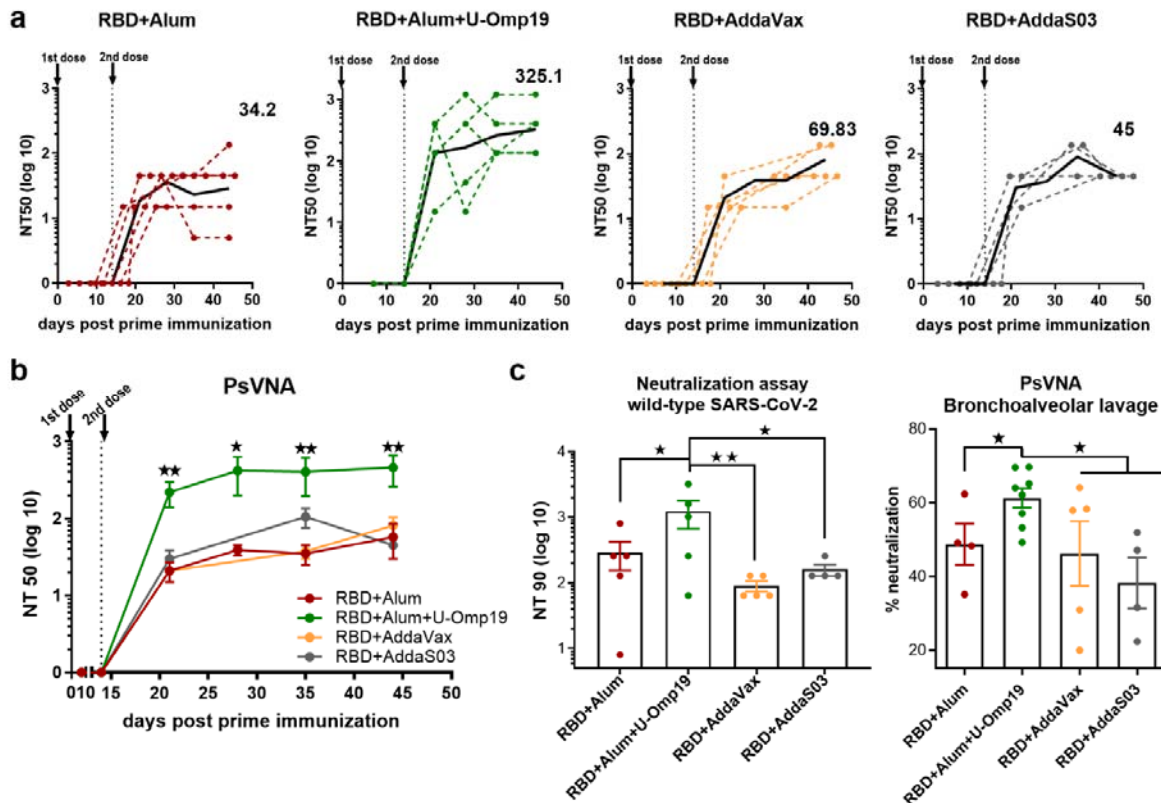
782 **Figure 2**



783  
784  
785  
786  
787  
788  
789  
790  
791  
792  
793  
794  
795  
796  
797  
798  
799  
800  
801  
802  
803

**Figure 2. BALB/c mice immunized with RBD plus different adjuvants induced RBD-specific antibodies.**  
**A.** Immunization protocol scheme. BALB/c mice were vaccinated at day 0 and day 14 via i.m. with: RBD+Alum (n=5), RBD+Alum+U-Omp19 (n=5), RBD+AddaVax (n=5) or RBD+AddaS03 (n=4). Serum samples were obtained at indicated time points for ELISA and neutralization assays. **B.** Kinetics of RBD-specific IgG endpoint titers in sera of immunized animals by ELISA. Points are means  $\pm$  SEM. **C.** RBD-specific IgG subclasses (IgG1 and IgG2a) titers in sera of immunized animals at day 42 post prime immunization. **D.** Detection of RBD-specific IgG and **E.** IgA in the bronchoalveolar lavage of immunized mice at day 42 post prime immunization. Data are optical density (OD) at 450nm. \*p<0.05. \*\*p<0.01. Mann Whitney test.

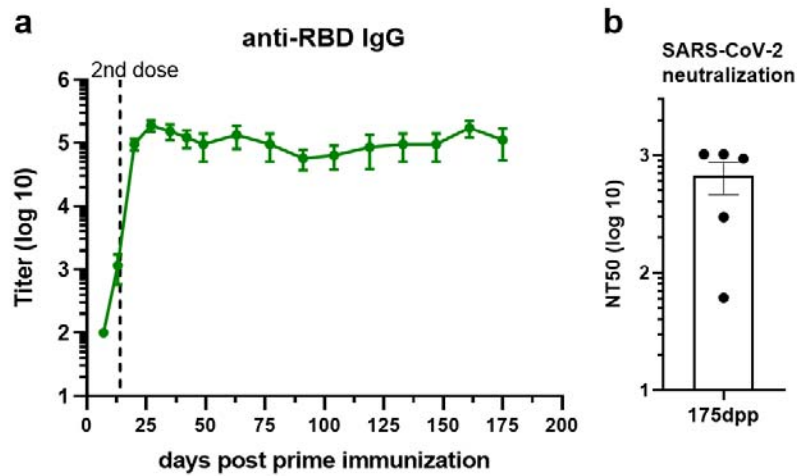
804 **Figure 3**



805  
 806 **Figure 3. Immunization with RBD+Alum+U-Omp19 increases systemic and mucosal neutralizing**  
 807 **antibody titers.** **A.** BALB/c mice were vaccinated as described in Fig. 2. Serum neutralizing-antibody titers  
 808 determined by pseudo-typed SARS-CoV-2 assay for each group of vaccinated mice at different time points.  
 809 The black lines represent the geometric mean of all data points and numbers are GMT on day 42. Dotted lines  
 810 represent the mean titer of each mouse at indicated time points. Titers correspond to the 50% of virus  
 811 neutralization (NT50). **B.** Kinetics of neutralizing antibody titers of all groups determined by pseudo-typed  
 812 SARS-CoV-2 assay. Points are Means  $\pm$  SEM. Titers correspond to the 50% of virus neutralization (NT50).  
 813 \* $p < 0.05$ . \*\* $p < 0.01$ . One way ANOVA with Bonferroni post-test. **C.** Neutralizing antibody titers against wild-type  
 814 SARS-CoV-2 virus at day 42 post prime immunization. Neutralization titer was defined as the highest serum  
 815 dilution without any cytopathic effect in replicable wells (NT 90). Data are shown as means  $\pm$  SEM. \* $p < 0.05$ .  
 816 \*\* $p < 0.01$ . One way ANOVA with Bonferroni post-test. **D.** Determination of neutralizing antibodies in the  
 817 bronchoalveolar lavage by pseudo-typed SARS-CoV-2 assay at day 42. Data are expressed in percentage of  
 818 neutralization compared with controls (virus alone). \* $p < 0.05$ . T test.

819  
 820  
 821  
 822  
 823  
 824  
 825  
 826  
 827  
 828  
 829

830 **Figure 4**



831 **Figure 4. RBD+Alum+U-Omp19 immunization induces a long-term antibody response. A.** Kinetics of  
832 RBD-specific IgG endpoint titers in sera of RBD+Alum+U-Omp19 BALB/c immunized animals by ELISA.  
833 Points are means  $\pm$  SEM. **B.** Bar plot of neutralizing-antibody titer against wild-type SARS-CoV-2 at day 175  
834 post prime immunization (dpp). Neutralization titer was defined as the serum dilution that reduces 50% the  
835 cytopathic effect (NT50). Data are mean  $\pm$  SEM.  
836

837

838

839

840

841

842

843

844

845

846

847

848

849

850

851

852

853

854

855

856

857

858

859

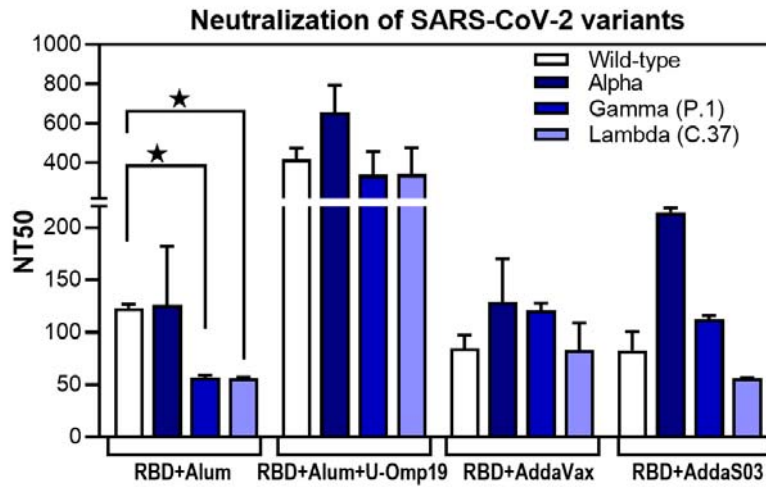
860

861

862

863

864 **Figure 5**

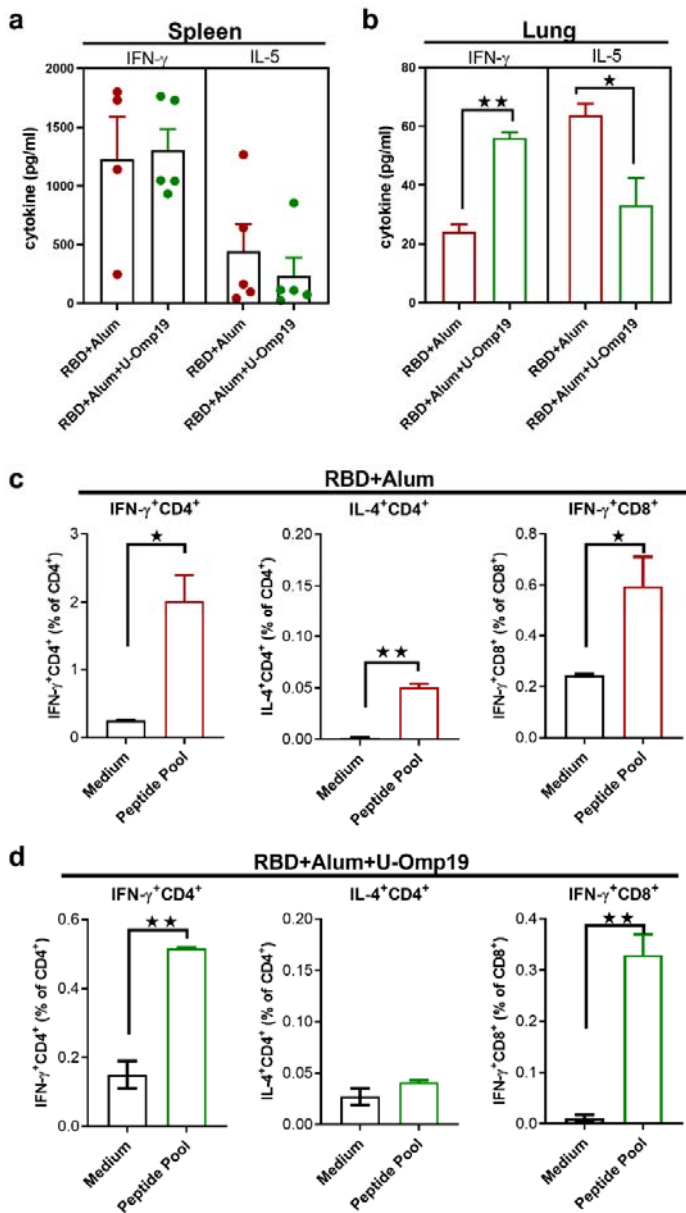


865 **Figure 5. U-Omp19+Ag+Alum formulation induces neutralizing Abs against multiple SARS-CoV-2**  
866 **variants.** BALB/c mice were vaccinated as described in Fig. 2. Neutralizing-antibody titers against ancestral  
867 (wild-type) SARS-CoV-2 and alpha, gamma (P.1) and lambda (C.37) variants were assessed one month post  
868 second dose. Neutralization titer was defined as the serum dilution that reduces 50% the cytopathic effect  
869 (NT50). Bars represent means  $\pm$  SEM. \* $p < 0.05$ . T test.

870  
871  
872  
873  
874  
875  
876  
877  
878  
879  
880  
881  
882  
883  
884  
885  
886  
887  
888  
889  
890  
891  
892  
893  
894  
895  
896  
897



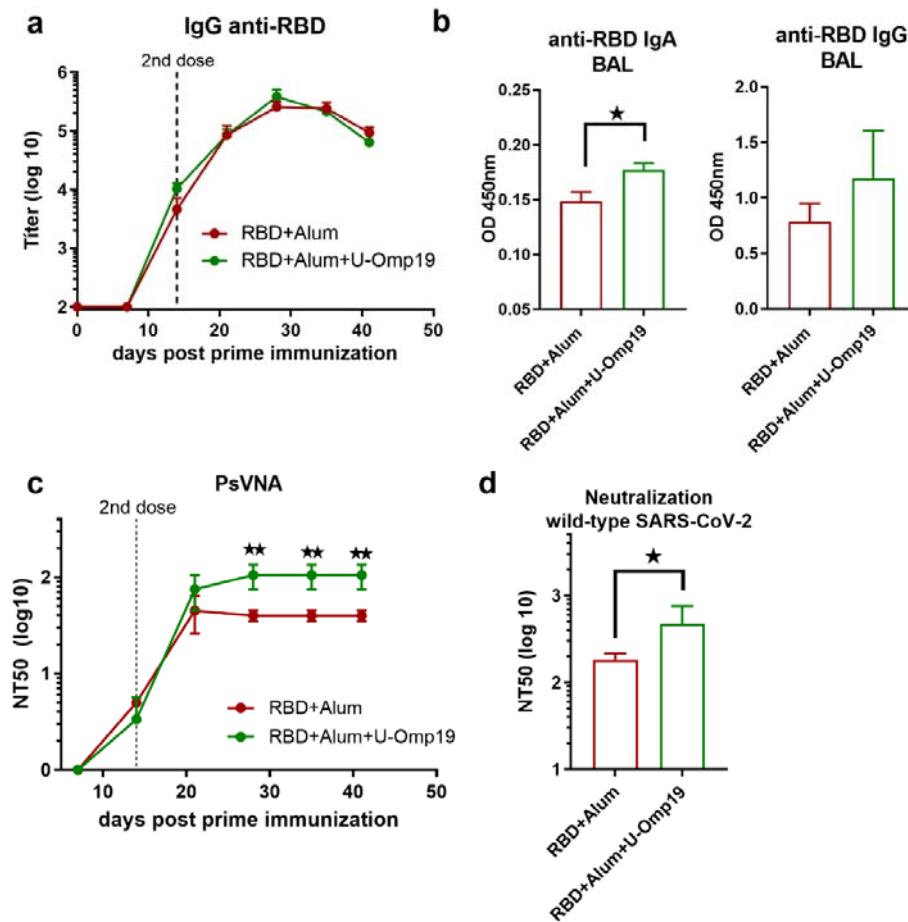
898 **Figure 6**



899 **Figure 6. U-Omp19+RBD+Alum formulation induces systemic and mucosal Ag-specific Th1 and CD8<sup>+</sup>**  
 900 **T cells.** BALB/c mice were vaccinated as described in Fig. 2. Mice were sacrificed 42 days after the first  
 901 immunization to obtain spleens and lungs and T cell response was evaluated. Levels of secreted IFN- $\gamma$  and  
 902 IL-5 following splenocytes (A) or lung cells (B) stimulation with medium or recombinant RBD were determined  
 903 by ELISA. Bars are means  $\pm$  SEM of pg/ml of IFN- $\gamma$  and IL-5 after subtracting the amount in medium  
 904 stimulated cells. \* $p$ <0.05, \*\* $p$ <0.01. T test. C,D. Intracellular flow cytometry analysis of cytokine secreting T  
 905 cells. Splenocytes from groups RBD+Alum (C) or RBD+Alum+U-Omp19 (D) were stimulated with complete  
 906 medium or RBD-peptides pool for 18 h and then brefeldin A was added for 5 h. Afterward, cells were  
 907 harvested and stained with specific Abs anti-CD8, and anti-CD4, fixed, permeabilized, and stained  
 908 intracellularly with anti-IFN- $\gamma$  and anti-IL-4. Results are presented as percentage of IFN- $\gamma$  or IL-4-producing T  
 909 lymphocytes. Bars are means  $\pm$  SEM. \* $p$ <0.05, \*\* $p$ <0.01 vs. medium. T test.

911  
 912

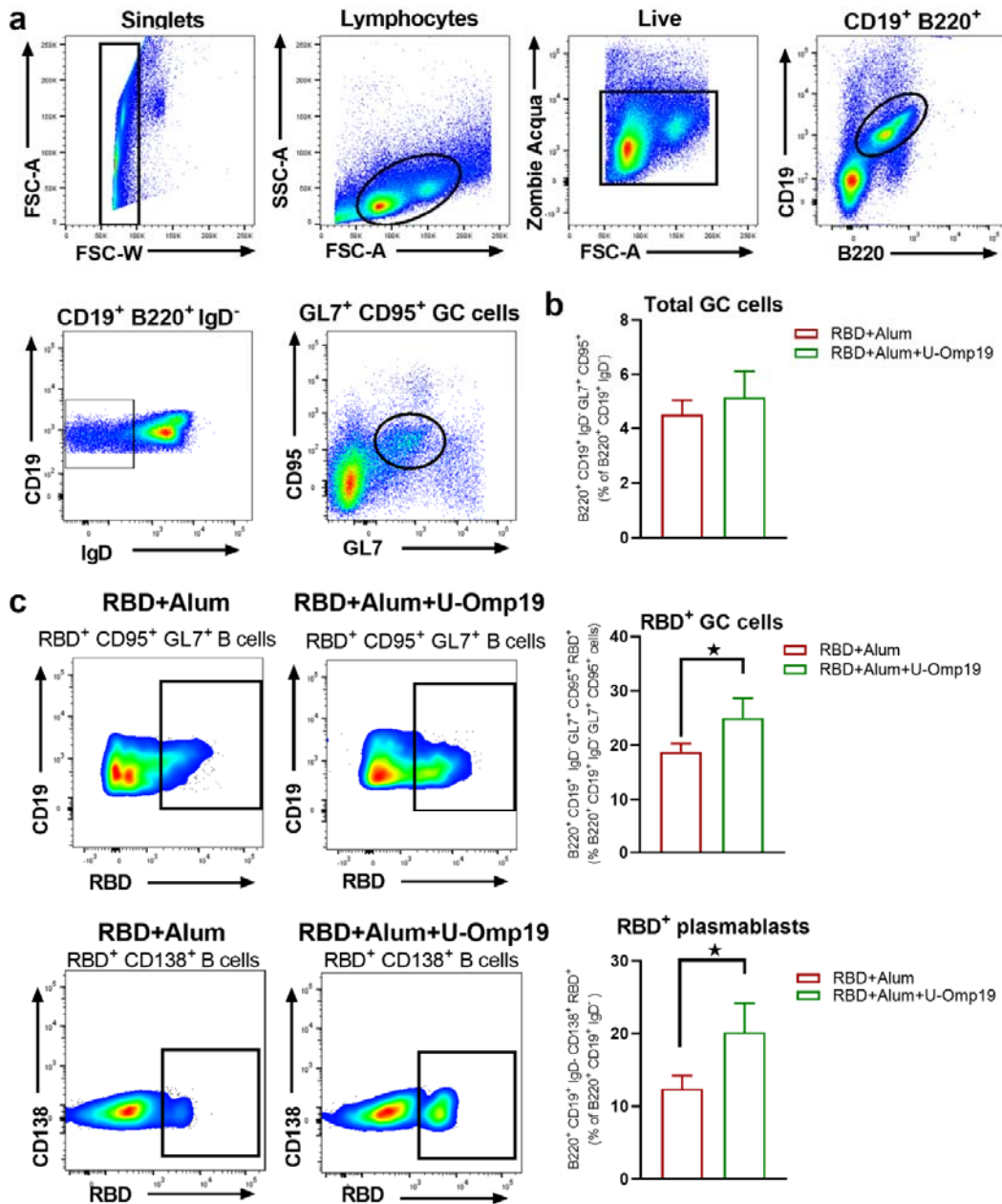
913 **Figure 7**



914  
915  
916  
917  
918  
919  
920  
921  
922  
923  
924  
925  
926  
927  
928  
929  
930  
931  
932  
933  
934  
935  
936

**Figure 7. U-Omp19 as adjuvant increases neutralizing antibodies in C57BL/6.** C57BL/6 mice were vaccinated at day 0 and day 14 via i.m. with RBD+Alum or RBD+Alum+U-Omp19. **A.** Kinetics of RBD-specific IgG endpoint titer in sera of immunized animals by ELISA. Points are means  $\pm$  SEM. **B.** Detection of RBD-specific IgA and IgG at the bronchoalveolar lavage of immunized mice at day 42 post prime immunization. Data are optical density (OD) at 450nm. \* $p < 0.05$ . Mann Whitney test. **C.** Kinetics of neutralizing-antibody titers determined by pseudo-typed SARS-CoV-2 assay. Neutralization titer was defined as the reciprocal serum dilution that causes a 50% reduction of transduction efficiency (NT50). \*\* $p < 0.01$ . T test. **D.** Neutralization titers against wild-type SARS-CoV-2 virus at day 42. Neutralization titer was defined as the serum dilution that reduces 50% the cytopathic effect (NT50). Data are shown as means  $\pm$  SEM. \* $p < 0.05$ . T test.

937 **Figure 8**



938

939

940 **Figure 8. U-Omp19 as adjuvant increases RBD specific germinal centers cells and plasmablasts.** Mice

941 were vaccinated as described in Fig. 7. Flow cytometry analysis of different B cell populations at spleen of

942 vaccinated mice were performed using, anti-CD19, anti-B220, anti-IgD, anti-CD138, anti-GL7 and anti-CD95

943 antibodies. Specific cells were determined by binding to fluorescent RBD. Gating strategy is shown in A. B.

944 Results are presented as percentage of total GC cells (B220<sup>+</sup> CD19<sup>+</sup> IgD<sup>-</sup> GL7<sup>+</sup> CD95<sup>+</sup>).

945 Bars are means ± SEM C. Dot plots for each group are shown (right) and results are presented as percentage of RBD-specific

946 GC cells (B220<sup>+</sup> CD19<sup>+</sup> IgD<sup>-</sup> GL7<sup>+</sup> CD95<sup>+</sup> RBD<sup>+</sup>).

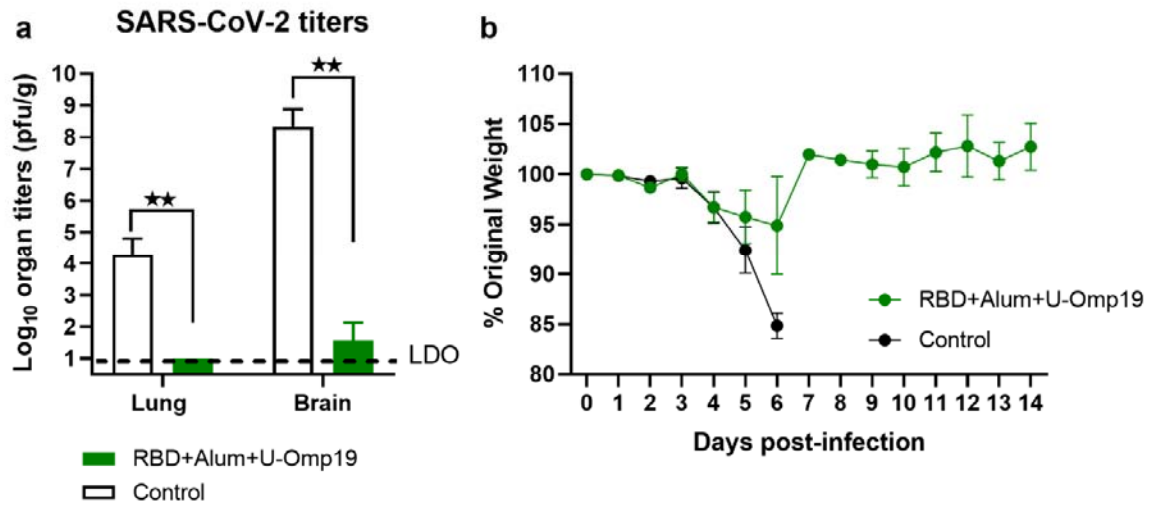
947 Bars are means ± SEM. \**p*<0.05. T test. D. Dot plots for each group are shown (right) and results are presented as percentage of RBD-specific plasmablasts (B220<sup>+</sup>

948 CD19<sup>+</sup> IgD<sup>-</sup> CD138<sup>+</sup> RBD<sup>+</sup>).

949 Bars are means ± SEM. \**p*<0.05. T test.

950

951 **Figure 9**



952

953

954 **Figure 9. Vaccination with RBD+Alum+U-Omp19 protects K18-hACE2 transgenic mice against SARS-**

955 **CoV-2 infection.** Mice received PBS (Control) (n=7) or RBD+Alum+U-Omp19 (n=8) administered via i.m.

956 route at day 0 and 14. Four weeks following immunization, K18-hACE2 mice were intranasally infected with  $2$

957  $\times 10^5$  PFU of SARS-CoV-2. Five days after infection lungs and brains (n=3) were obtained from groups of

958 mice and SARS-CoV-2 virus was titrated. Bars represent the mean  $\pm$  SEM. Dotted line: limit of detection

959 (LOD). \*\*p<0.01. T test. **(B)** Weight loss outcomes in K18-hACE2 transgenic mice vaccinated and challenge

960 with SARS-CoV-2. Weight changes in mice were monitored daily until day 14 after infection. Points are means

961  $\pm$  SEM of percentage of original weight.

962